RELIABILITY ANALYSIS OF GREEN ROOFS UNDER DIFFERENT STORM SCENARIOS

BY

RESHMINA WILLIAM

THESIS

Submitted in partial fulfillment of the requirements
for the degree of Master of Science in Civil Engineering
in the Graduate College of the
University of Illinois at Urbana-Champaign, 2015

Urbana, Illinois

Advisor:

Assistant Professor Ashlynn S. Stillwell

ABSTRACT

The rise of urban environments has created issues with localized flooding and water quality due to changes in runoff caused by increasing impervious area. Green infrastructure offers an alternative method of runoff reduction, by using natural processes to infiltrate, store, and treat runoff at its source. In particular, green roofs can promise multiple benefits in terms of runoff reduction, air quality improvement, and mitigation of the urban heat island effect, while taking up little additional land. However, few consistent standards exist to help designers and planners decide whether or not a green roof is performing as expected. This research provides a reliability analysis-based methodology that can be used to evaluate green roof runoff reduction. Green roof failure is characterized using a visual aid typically used in earthquake engineering: fragility curves. The 2D distributed surface water-groundwater coupled program MIKE SHE was used to model the runoff from a simple intensive green roof located on the University of Illinois at Urbana-Champaign (UIUC) campus under different storm scenarios. The results from these runs were then input into the reliability analysis software FERUM in order to calculate the probability of failure under the first order reliability method (FORM), second order reliability method (SORM), and Monte Carlo analyses. The fragility curves generated show the efficiency in runoff reduction provided by a green roof compared to a conventional roof under different storm scenarios. The use of reliability analysis as a part of green roof design code can help test for weaknesses and areas for improvement pertaining to peak runoff reduction. It can also help to support the design of code that is more resilient and testable for failure than current standards.

ACKNOWLEDGMENTS

I would like to thank DHI Water and Environment for providing the student license for my use of MIKE SHE in this thesis. I would also like to thank Professor Paolo Gardoni for his help in adapting the fragility curve framework that is used for this analysis, and Professor Art Schmidt for his help and advice in using MIKE SHE to model green infrastructure.

I would like to thank my family and friends in the Ven Te Chow Hydrosystems Lab for their help and support. I would particularly like to thank Nathanial Hanna Holloway and Najwa Obeid for their help in data collection from the Business Instructional Facility (BIF) green roof, and Viviana Fernanda for her help in data processing. Finally, I would like to thank the other members of the Stillwell Research Group for their suggestions, support, and guidance throughout the design and writing process.

Funding for this thesis was provided through the Kinra and CEE Distinguished Fellowships.

Table of Contents

CHAPTER 1: Introduction

The issue of urban stormwater has become increasingly pertinent in the developed world, with major cities across the globe seeking technological 'silver bullets' to the twin threats of flooding and water contamination. Urbanization has led to a rapid increase in the area of impermeable surface within watersheds. The excess runoff generated by additional impermeable surface can cause extensive flooding and erosion due to the high velocity of the water channeled off roads and rooftops. Urban stormwater also generates non-point source pollution issues, ranging from sediment overloading in rivers and streams to contamination from antifreeze, oil, and heavy metal particulates washed off roads (CWEP, 2015). Older cities such as Chicago present additional challenges: because of their combined sewer systems, excess stormwater can lead to combined sewer overflows (CSOs), which wash untreated sewage into watercourses such as the Chicago River (MWRD, 2014).

Green infrastructure has been touted as an effective solution to the problems created by increased stormwater runoff. In particular, it has been suggested as a feasible alternative to traditional 'gray infrastructure' (engineered) treatment. Green infrastructure makes use of natural processes provided by vegetation and soil to filter and store excess water (CNT, 2010). For older, more established cities, the development of green belts or rain gardens at ground level might not be a feasible alternative, particularly in areas that already have significant infrastructure in place. Green roofs provide an attractive alternative for highly urbanized areas by making use of an under-utilized and highly impervious area of residential and industrial buildings: the roof. From Chicago to Zurich, from Hong Kong to London, green roofs are anticipated to help provide an inexpensive solution to many of the pollution and environmental degradation issues facing large cities (Klinkenborg, 2009).

However, the efficiency of green roofs in reducing peak hydrograph flow is characterized by wide variability and uncertainty. In their review paper, Li and Babcock (2014) indicated that green roofs reduce peak flow rates by between 22 and 93%, indicating deep uncertainty in green roof performance. Among other factors, green roof runoff

reduction is affected by vegetation type, planting medium depth and type, antecedent moisture conditions, and the intensity and duration of storm events. Literature reporting which factors are most important for smaller storms versus larger ones, or how sensitive existing model parameters are to change, is sparse. Because of the nascent nature of green infrastructure as a method for regulating peak discharge, there are few national codes that specify threshold efficiency for green roofs. While the Municipal Water Reclamation District of Greater Chicago (MWRDGC) has defined some guidelines for green infrastructure design, these guidelines are based off volumetric detention rather than peak runoff (State of Illinois v. MWRDGC, 2014). The Illinois Environmental Protection Agency (IL-EPA) (2010) report on green infrastructure efficiency compiled suggested recommendations at the county level in an attempt to create a coherent set of standards for Illinois as a whole (Jaffe et al., 2010). The recommendations for peak discharge generally suggest a maximum allowable runoff of 0.04 cubic feet per second (cfs)/acre for the 2-year, 24-hour storm and 0.1 cfs/acre for the 100-year, 24-hour storm.

These recommendations, however, are static in time; they do not allow a comparative approach to green roof evaluation in the context of different design storms. According to studies conducted by Holmann-Dodds et al. (2003), green infrastructure is most effective for smaller-scale storms that mostly produce runoff from impervious areas with minimal runoff from pervious areas. Studies have been conducted in the field investigating the reduction of runoff, improvement in water quality, and increase in storage created by different types of green infrastructure under different storms (Davis, 2008; Dietz and Clausen, 2005). However, a probabilistic analysis of green infrastructure 'failure' independent of storm intensity has not yet been attempted, to the author's knowledge.

An alternative analysis framework is suggested, which makes use of reliability analysis tools to create fragility curves, which create a visual reference of the probability of failure of a system or component under different forcing intensities. Bai et al. (2009) investigated the use of fragility curves in comparing the probability of failure of a building under different damage criteria (ranging from insignificant to critical damage) and different earthquake intensities. In this work, a similar approach is suggested in investigating the efficiency of green roofs in reducing peak runoff compared to storms of different return

periods. This work presents a quantitative reliability analysis-based assessment of green roof failure under different storm scenarios. As such, it aims to answer the following motivating research question:

How might we quantify the efficiency in peak runoff reduction of green roofs?

In answering this research question, this thesis is organized as follows: Chapter 2 presents background on green infrastructure and green roofs in particular; Chapter 3 describes materials and methods for quantifying peak runoff from green roofs; Chapter 4 describes details of reliability analysis; Chapter 5 presents results of green roof modeling efforts and fragility curves; Chapter 6 provides policy implications and broader context; and Chapter 7 summarizes high-level conclusions.

CHAPTER 2: Background

The traditional approach to runoff management and control has been to consider stormwater as a resource that has no value, "is environmentally benign, and adds little to the amenity… of an urban environment" (Wong, 2006). This attitude has created a system of highly efficient engineered drainage systems to collect and rapidly remove stormwater. The increased runoff rates and 'flashy' hydrographs created by urban development have created issues with flooding, erosion, and water quality. In contrast, green infrastructure aims to foster "an interconnected network of natural areas… that conserves ecosystem values and functions, sustains clean air and water, and provides a wide array of benefits to people and wildlife" (Benedict and McMahon, 2006). In other words, the main focus of green infrastructure is the integration of natural elements that help to provide key ecosystem services (The Conservation Fund, 2011). The umbrella title of 'green infrastructure' encompasses a wide range of engineered and non-engineered practices including rain gardens, bioswales, permeable pavements, and green roofs.

Multiple studies indicate that a combination of green and gray (traditional) infrastructure is critical to expanding existing sewer services at a reasonable cost without creating adverse environmental impacts. In particular, Wang et al (2013) suggest that implementing a combined green infrastructure approach before the construction of gray alternatives (such as separated sewers) leads to better overall local water quality. However, they also note that increased imperviousness and higher local rainfall intensity can seriously constrain the effectiveness of green infrastructure. The changes imposed by climate change and increasing urbanization mean that a combination of green and gray infrastructure changes is likely needed for sustainable urban development. Just as importantly, an understanding of the long-term reliability of different green infrastructure components is also required to better integrate them into existing sewer designs. Real-life monitoring studies conducted in New York City indicate that green infrastructure can play a significant role in reducing stormwater runoff and improving water quality in a highly urbanized environment (City of New York DEP, 2015).

According to the Center for Neighborhood Technologies (CNT) 2010 Guide to Green Infrastructure, a green roof is "a rooftop that is partially or completely covered with a growing medium and vegetation planted over a waterproofing membrane". Green roofs typically also include root barriers, drainage, and irrigation features, as illustrated in Figure 1. There are two main types of green roofs, as characterized by the depth of the planting media: extensive (two – six inches), and intensive (over six inches) (Oberndorfer et al., 2007). Plant species selected for green roofs are typically native to the local environment, and can have additional beneficial properties such as drought resistance. Species are typically chosen to avoid the need for irrigation (Dunnett and Kinsbury, 2008). Sedums and other succulents are typical choices for extensive green roofs due to their drought-resistance, ability to store moisture, and shallow taproots (Dunnett and Nolan, 2004; Getter and Rowe, 2008). However, researchers are investigating the viability of over 100 native and non-native plant species for extensive, semi-intensive, and intensive green roofs at the Chicago City Hall green roof. This increased variety in rooftop plants is desirable as a source of increased biodiversity and an attraction to pollinators such as bees (Yocca, 2002). Evidence shows that improved biodiversity does somewhat improve the survival of plant species besides grasses and forbs (Nagase and Dunnett, 2010).

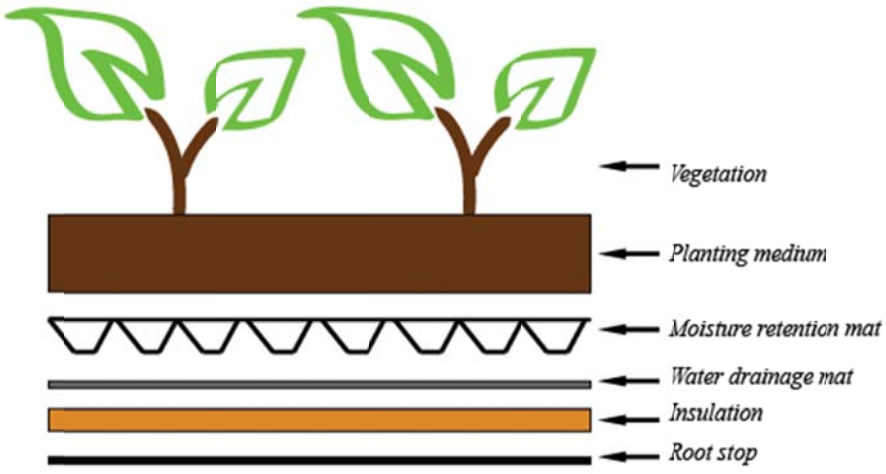

Figure 1. This diagram of the University of Illinois Business Instructional Facility green roof shows the layout of a typical green roof (based on Hanna Holloway et al., 2009).

Green roofs have been repeatedly proven to have multiple useful benefits in terms of ecological function, air and water quality, temperature control, roof maintenance, and runoff reduction (Oberndorfer et al., 2007). Up to 32% of the horizontal surface of a typical built-up area can be rooftops, making green roofs a potentially valuable addition to a properly managed urban environment (Frazer, 2005). Vegetation helps to eliminate air-borne pollutants through the uptake of chemical compounds through their stomata, interception of particulates with their leaves, and the breakdown of organics in plant tissue. In fact, it is estimated that nitrous acid – a form of dissolved nitrogen – can be reduced by as much as 21% above a green roof (Rowe, 2011). Air quality is also improved by the decrease in building temperatures that occurs around green roofs, enabling better air flow and mixing in the surrounding areas (Baik et al., 2012). The impact of green roofs on the urban head island effect can be significant, helping to decrease ambient air temperatures on a large scale (Gagliano et al., 2015; Santamouris, 2015). Green roofs have also been proven to help reduce building energy costs by reducing cooling requirements within the building during peak summer conditions (Niachou et al., 2001; Virk et al., 2015).

Green roofs are particularly valuable in densely populated urban environments because they do not require the large amounts of space needed for traditional gray infrastructure, such as storage reservoirs and ponds (Mentens et al., 2005). Green roofs capture stormwater during rainfall events within their porous soil planting medium. Extensive green roofs have been shown to effectively act like storage reservoirs, capturing water until the soil was saturated, and then releasing water in a manner similar to a traditional roof (Carter and Rasmussen, 2006). Green roofs can retain anywhere between 40 to 80% of annual precipitation (CNT, 2010). Indeed, research on experimental plots in Atlanta, Georgia, indicates that green roofs effectively capture the majority of runoff from smaller storms (Carter and Rasmussen, 2006). Green roofs also help to decrease net runoff volume by storing and releasing water to the atmosphere via plant evapotranspiration. During the summer, up to 15 cm evapotranspiration has been observed from green roof experimental research stations (Marasco et al., 2014). Besides simply increasing overall storage capacity and reducing runoff volume, green roofs help to delay peak storm runoff, significantly reducing the risk of overloading existing stormwater conveyance facilities (Mentens et al.,

2005; Moran et al., 2005; Getter and Rowe, 2006). Green roofs can delay peaks from between 1.5 to 4 hours, compared to roofs with no vegetation. Reducing and delaying the stormwater peak also helps to reduce overall flows off the roof, sometimes by as much as 87% (Getter and Rowe, 2006).

Various theoretical studies indicate that green roofs can effectively help to mitigate the negative impacts of increasing impervious area due to urbanization. Carter and Jackson (2007) created a simple hydrologic model using experimental data collected from real green roofs. This model was used to study the impact of multiple green roofs in and urban environment. At the basin scale, runoff reduction can approach 35% when all available surfaces are converted into green roofs. Consequently, green roofs can be a significant supplement to the storage capacity of traditional gray infrastructure. Deutsch et al. (2005) concluded that if 20% of the suitable buildings in Washington D.C. hosted a green roof, the city would increase its stormwater storage capacity by almost 71 million L.

However, these stormwater benefits can vary widely. According to Getter and Rowe (2006), green roofs can effectively reduce runoff by 60 to 100%. Li and Babcock (2014) state that lab and field experiments have shown that green roofs can reduce runoff volume by 30 to 86% and reduce peak flow rate by 22 to 93%. The large amount of variability in green roof efficiency is caused by a variety of factors. Analyses conducted by Holman-Dodds et al. (2003) show that both the impact of urbanization and the mitigating potential of low impact developments (LIDs) are dependent on the underlying soil texture. In addition, they conclude that mitigation is strongly dependent on storm size. LIDs typically show the greatest mitigating ability for smaller storms with shorter return periods (Holmann-Dodds et al., 2003; Carter and Rasmussen, 2006; Davis, 2008). LIDs can completely compensate for development in areas with highly infiltrative soils for events that deposit less than 1 inch of rainfall. However, LID capabilities are greatly reduced during high intensity events. Antecedent soil moisture conditions and inter-storm duration also play important roles in green roof runoff reduction (Carter and Rasmussen, 2006; Davis, 2008).

A series of experiments carried out by Davis (2008) on bioretention cells support these conclusions. In almost one-fifth of the observed cases, the storm events were small enough that the entire inflow volume was captured. In other events, typical flow peak

reductions of up to 63% were noted. However, the same impacts of soil type and storm size were noted. The antecedent conditions of the bioretention cell were also found to have an impact on hydrological performance. While the effect for larger storms was minimal, antecedent moisture conditions had a significant effect for smaller storms. Similarly, Wilson et al. (2015) noted that large reductions in peak flow in a green-gray combined system could be the result of a significantly over-designed system, coupled with highly permeable local soils.

Roof slope and media depth also have significant impacts on the efficiency of green roofs in particular (VanWoert et al., 2005). Decreasing roof slope helps to increase the amount of water retained on the roof surface, thus helping to reduce peak runoff volume. Similarly, deeper media green roofs create a larger retention area for water, helping to reduce the hydrograph peak. Experimental studies also indicate that the addition of vegetation both reduces the total amount of stormwater runoff and extends hydrograph duration. However, the impact of the vegetation itself is fairly small compared to the effects of the growing media depth and type (VanWoert et al., 2005).

Drought stress can also impact green roof efficiency. Indeed, some predictions show green roof runoff increasing by as much as 50% in the future as a result of vegetation stress induced by climate change, although certain plant species will likely be more affected than others (Vanuytrecht et al, 2013). Vanuytrecht et al. (2013) investigated the drought stress and runoff from green roofs containing grass-herb and sedum-moss vegetation under different current and predicted climate scenarios. Overall, drought stress of the herb-grass roofs was more than twice that of the sedum-moss roofs. However, stormwater runoff reduction was higher on grass-herb roofs than on sedum-moss roofs, demonstrating a tradeoff between drought resilience and runoff reduction. Vanuytrecht et al. (2013) concluded that this tradeoff should be considered in the choice of plants for green roofs.

Because of variations in climate, vegetation, and soils, green infrastructure is not easily implemented using a ‘one-size-fits-all’ methodology developed for the entire country. Gallo et al (2012) suggest that although LIDs are effective to some extent in all areas of the country at managing small events, their relative impacts can vary widely. Furthermore, the ability of LIDs to manage large return-period events changes drastically from one part of the

country to the next. For instance, Portland, Oregon, has both smaller and less intense storms than most cities, making LIDs more effective in managing the city's largest storm events. However, changing the designed infiltration rate of the soil mix could significantly impact the ability of different regions to manage storms.

Multiple computer modeling studies have been created to analyze the ability of green roofs to manage stormwater. Models run the range from simple water-balance analyses to 1-D modeling studies to 2-D integrated flow mapping (Jarrett et al, 2007; Hilten et al., 2008; Jaber and Shukla, 2012; Obeid, 2014; William and Schmidt, 2015). Researchers at Pennsylvania State University used a simple spreadsheet approach to model the retention of stormwater on a green roof at an annual time-step, investigating the impact of the planting medium thickness on annual stormwater retention (Jarrett et al., 2007). Several studies have used the 1-D modeling program HYDRUS to accurately simulate green roof performance. Hilten et al. (2008) used HYDRUS to test the performance of a single modular green roof to simulate runoff based on climatic data collected from Athens, Georgia. The study confirmed that the rainfall depth strongly influences the performance of green roofs, although a rigorous reliability analysis was not conducted based on the results. Similarly, Obeid (2014) used outputs from a HYDRUS 1-D model calibrated using data from Champaign, Illinois, to understand the impact of green roofs on runoff processes at a watershed scale.

The more complex 2-D distributed coupled surface water-groundwater model MIKE SHE has been used to inform several studies in the fields of water resources and sustainability (Jaber and Shukla, 2012; Choi and Schmidt, 2013; William and Schmidt, 2015). More directly, MIKE SHE can be used to incorporate spatial elements into the modeling of green infrastructure on a larger scale. Christensen (2006) used MIKE SHE and its associated river routing program, MIKE 11, to analyze the impact of sizing and distribution of rain gardens within an urban environment. Similarly, Trinh and Chui (2012) used MIKE SHE to simulate the impact of urban restoration on peak runoff and runoff magnitude. This analysis employs MIKE SHE to model a single green roof in a modular fashion that can be integrated into a larger network analysis framework. Using techniques from reliability analysis to generate fragility curves creates the opportunity to better

understand the effects of green roof variability on runoff mitigation, as well as to focus on how green roof designs can be improved.

CHAPTER 3: Material and methods

3.1 General methodology

To create the fragility curves for a single green roof, data from a green roof located on the University of Illinois at Urbana-Champaign (UIUC) campus was used as a model input. Data on vegetation and soil characteristics, weather, and runoff were input into the modeling software MIKE SHE. The MIKE SHE model was then calibrated using data taken from high intensity short duration storms, and from low intensity long duration storms. The calibration was based on matching the hydrograph peak and the rising limb of the hydrograph rather than the tails, since peak runoff was the focus of the analysis. The calibrated model was then used to generate output hydrographs for 26 different variable scenarios under different storm events. Regression analysis was used to create an algebraic expression relating the runoff from the green roof to the different variables being considered for each storm (the "demand"). At the same time, a version of the MIKE SHE model with parameters similar to impervious cover was used to simulate the runoff that would occur on the conventional roof (the "capacity"). Finally, the demand function, capacity, and variable uncertainty analysis were input to the MATLAB-based reliability analysis model FERUM to calculate the probability of failure using FORM, SORM and Monte Carlo simulation. Figure 2 shows a diagram of the general methodology. It is important to note that this method is flexible: it can be adapted for different types of green infrastructure and use different models to simulate green infrastructure. Although MIKE SHE was chosen in this case, other models could also be used. MIKE SHE was employed in this case because the program is easily scalable to larger scenarios.

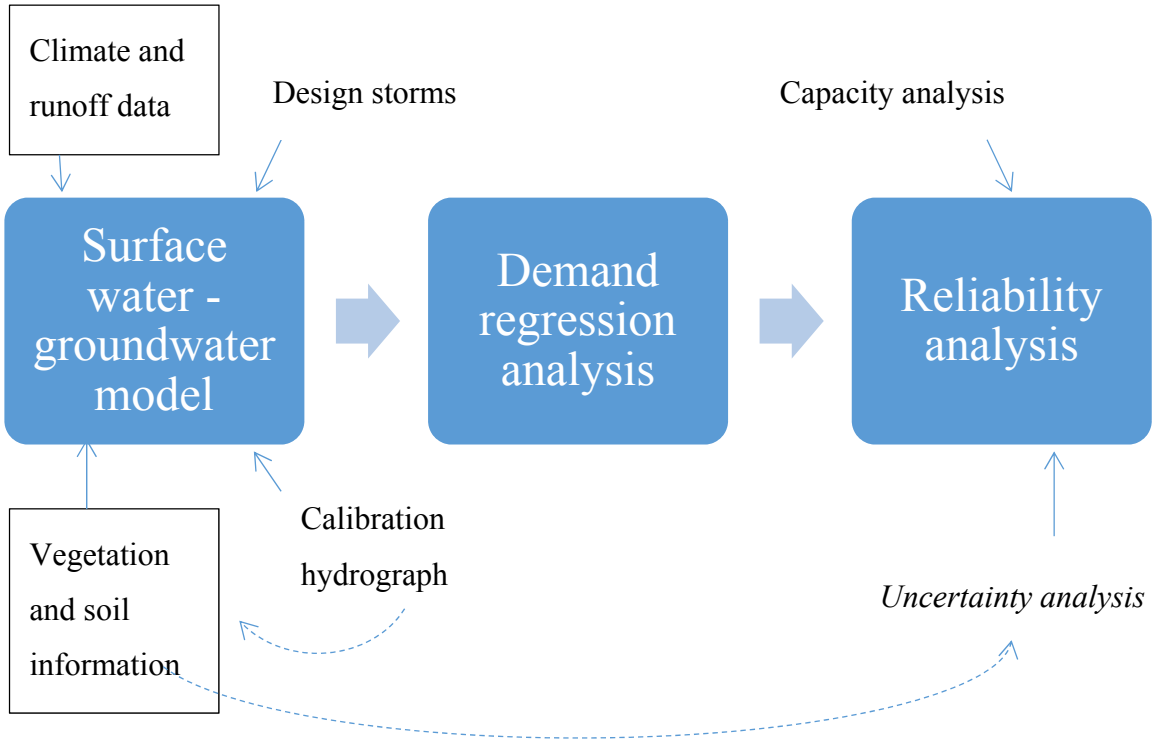

Figure 2. The modeling effort combined hydrologic data with vegetation parameters to model demand (runoff from the green roof). Reliability analysis combined the modeled demand functions with analysis of capacity (runoff from a simulated conventional roof) to determine the probability of failure.

3.2 Study location and monitoring system

Located on the south side of the UIUC campus, the Business Instructional Facility (BIF) prides itself on being one of the first LEED platinum certified buildings on campus. One component of the building's green vision was the development and implementation of a green roof on the east side of the building, as shown in Figure 3. Commissioned in late 2008, the roof is comprised of four monolithic vegetated beds that cover a total of 4000 ft^2. Each of the beds contains nine species of sedums, herbaceous plants, and native grasses as shown in Table 1. The roof was intended to both count towards the building's LEED accreditation and allow for the continued monitoring and scientific study of the roof over time (Hanna Holloway, 2009; Hanna Holloway et al., 2009; Obeid, 2014). For this reason, the roof was

equipped with a range of sensors to measure temperatures, water quality, soil moisture, and radiation.

Table 1. Many plant species are found on the Business Instructional Facility green roof at the University of Illinois at Urbana-Champaign.

Name	Common Name	Plant type
Allium Cernuum	Nodding wild onion	Grass
Buchloe Dactyloides 'Sharps Improved'	Buffalo grass	Grass
Dianthus Deltoides	Maiden pink	Herbaceous perennial
Koeleria Glauca	Prairie June grass	Grass
Sedum Acre	Goldmoss stonecrop	Sedum
Sedum Kamtschaticum	Stonecrop	Sedum
Sedum Spurium 'Bailey's Gold'	Bailey's gold stonecrop	Sedum
Sedum 'Ruby Glow'	Ruby glow stonecrop	Sedum
Thymus Serphyllum 'Coccineus'	Creeping thyme	Herbaceous perennial

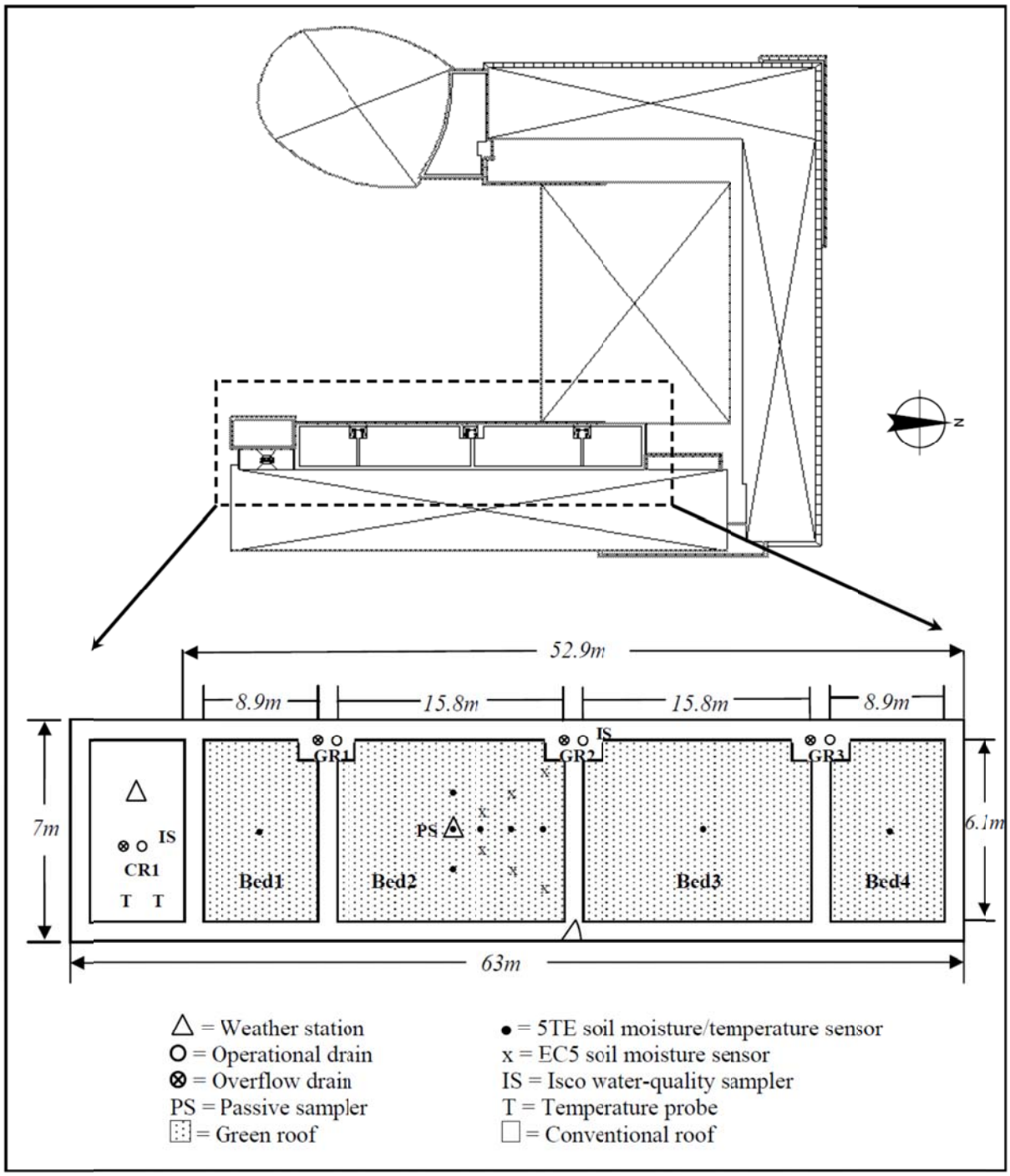

Figure 3. This plan view diagram of the Business Instructional Facility green roof shows the locations of sensors (reproduced from Holloway, 2009) [courtesy of UIUC campus Facilities and Services].

The planting medium depth is 20 cm (8 inches), meaning the roof is classified as intensive. However, the monolithic structure and lower maintenance needed for this roof causes it to be further classified as simple intensive. The planting medium is engineered LiteTop™ media with specifications as shown in Table 2. Sensors on the green roof measure air temperature, humidity, wind speed, rainfall, incoming and reflected radiation, and volumetric moisture content. An additional conventional roof is located 4.3 m above the green roof and hosts an additional weather station, water-quality sampler, and temperature probes, as well as pressure transducers for measuring runoff. Further details of the placement and calibration of the sensors can be found in Hanna Holloway et al. (2009).

Table 2. The green roof planting medium LiteTop™ has a range of physical properties [data courtesy of American Hydrotech, Inc.].

Grain Size Distribution	
clay fraction	< 1 %
passing #200 sieve	1-3 %
passing #60 sieve	5-25 %
passing #18 sieve	20-50 %
passing 1/8-inch sieve	55-95 %
passing 3/8-inch sieve	90-100 %
Density	
Application Density	0.6 - 1.1 g/cm^3
Saturated Density	0.9 - 1.4 g/cm^3
Dry Density	0.5 -1.0 g/cm^3
Water & Air Management (% vol.)	
saturated water capacity	>30 %
saturated air content	>10 %
Saturated Hydraulic Conductivity	>0.6 mm/min

3.3 Data processing

3.3.1 Precipitation

On the BIF green roof, precipitation is measured using a tipping bucket gage. As a result, the one-minute interval data collected by the precipitation gage on the green roof essentially measure the amount of time it takes to collect 0.1 inches of rainfall. However, the intensity, or precipitation rate, is the required input to MIKE SHE. To calculate the intensity (i), a simple conversion can be used as shown in Equation 1, where ΔP is the change in precipitation collected over a given time Δt.

$$i = \frac{\Delta P}{\Delta t} = \frac{P_2 - P_1}{t_2 - t_1} \quad \text{Equation 1}$$

3.3.2 Evapotranspiration

Reference evapotranspiration (ET) was calculated using the Food and Agriculture Organization (FAO) approximation of the Penman-Monteith equation (FAO, 2015) as shown in Equation 2.

$$ET_0 = \frac{0.408\Delta(R_n - G) + \gamma \frac{900}{T + 273} u_2 (e_s - e_a)}{\Delta + \gamma(1 + 0.34u_2)} \quad \text{Equation 2}$$

where ET_0 is reference evapotranspiration [mm/day]; R_n is net radiation at the crop surface [MJ/m^{2}day]; G is the soil heat flux density [MJ/m^{2}day]; T is the air temperature [°C]; u_2 is the wind speed at 2 m height [m/s]; e_s is the saturation vapor pressure [kPa]; Δ is the vapor pressure curve slope [kPa/°C]; and γ is the psychrometric constant [kPa/°C]. Evapotranspiration calculations using the mean flux profile, eddy covariance, or Bowen ratio method are in general more accurate than the Penman-Monteith equation in Equation 2, especially for surfaces that are not well-watered (e.g., completely wet). However, the FAO Penman-Monteith method allows for greater flexibility in gap-filling missing data without loss of overall accuracy. Overall, American Society of Civil Engineers (ASCE) and European studies have indicated that the FAO Penman-Monteith method is relatively accurate and consistent in both arid and humid environments (FAO, 2015). Although the equation best

describes evapotranspiration from a uniform well-watered grassy surface, it is considered acceptable for the purpose of calculating reference ET as an input for the MIKE SHE model. The reference ET is then used in conjunction with information about vegetation rooting depths and leaf area index (LAI) to compute the true ET, as discussed in Section 3.4.1.

The soil heat flux (G) can be calculated for each time-step from data collected from the soil temperature probes on the BIF green roof as described in Equation 3. The saturated vapor pressure (e_s) is calculated as a function of air temperature as described in Equation 4. As described in the FAO guidelines, the actual vapor pressure can be calculated as shown in Equation 5. Finally, the relationship between windspeed at a given measured height (h) and u_2 is given in Equation 6. Data taken from the Champaign 9 SW Station within the National Oceanic and Atmospheric Administration (NOAA) Quality Controlled Local Climatic Data database (NCDC, 2014) were used to gap-fill missing windspeed data.

$$G = \frac{\rho c d \Delta T}{\Delta t} \quad \text{Equation 3}$$

where ρ is the soil density;

c is the specific heat capacity;

d is the soil depth;

ΔT is the difference in soil temperature within time Δt

$$e_s = 0.6108 e^{17.27T/T+237.3} \quad \text{Equation 4}$$

where T is the air temperature in °C

$$e_a = RH \frac{e_s}{100} \quad \text{Equation 5}$$

where RH is the percent relative humidity

$$u_2 = \frac{4.87 u_h}{\ln(67.8h - 5.42)} \quad \text{Equation 6}$$

where u_h is the windspeed at height h above the ground

3.4 Modeling in MIKE SHE

MIKE SHE is a 2D distributed surface water-groundwater coupled modeling program. Modeling inputs are required to accurately model evapotranspiration (*ET*), infiltration and percolation, root uptake, subsurface flow, and drainage. Precipitation can be input as a uniform or spatially distributed time series by the user. ET inputs include net radiation (*Rn*), wind speed (*u*), vegetation leaf area index (*LAI*) and rooting depth (*RD*), soil and air temperature (*T*), and relative humidity (*RH*). The horizontal and vertical hydraulic conductivities of the LiteTop™ ($k_{LiteTop}$), gravel (k_{gravel}), and water retention panel (k_{ret}) are needed for infiltration and subsurface flow. Finally, the initial water table height (related to soil moisture content) (*h*), the drainage elevation, and the drainage constant (C_{drain}) are required for the model to accurately model outflow from the system. Figure 4 shows a diagram of MIKE SHE inputs.

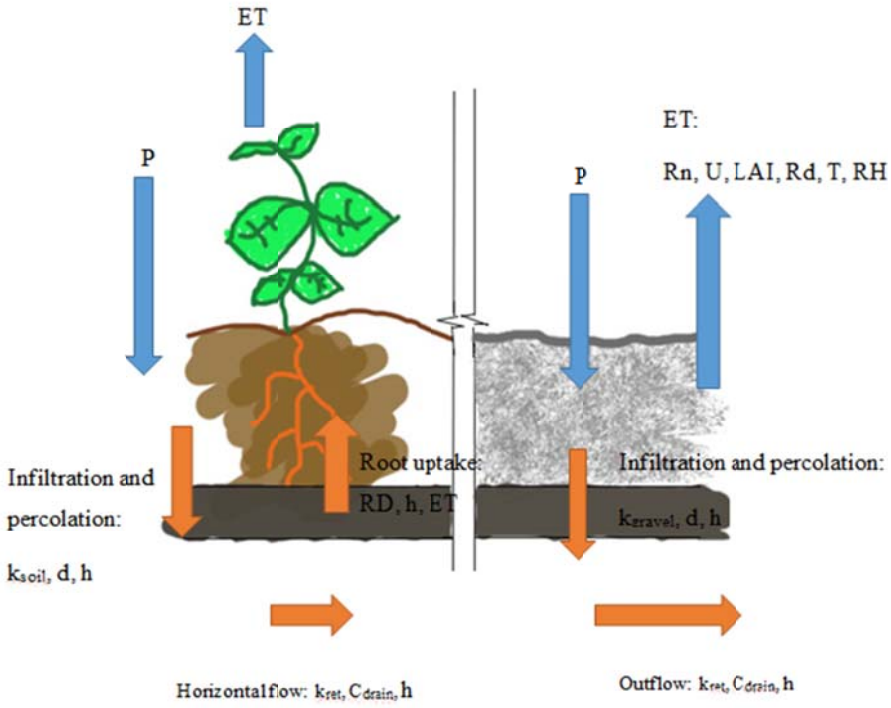

Figure 4. Inputs to the MIKE SHE model include evapotranspiration variables and soil and vegetation parameters.

While MIKE SHE has been used for both large scale (William and Schmidt, 2015) and small scale (Choi and Schmidt, 2013) modeling of diverse watersheds, it is not appropriate for analyzing small scale pore processes. In characterizing the coupling between surface water and groundwater in a green roof, MIKE SHE remains a useful and appropriate tool.

3.4.1 Evapotranspiration

To model evapotranspiration (ET) in MIKE SHE, the reference evapotranspiration, leaf area index (LAI) and plant rooting depth (RD) must be known. Plant-based ET is modeled using an empirical formula developed by Kristensen and Jensen (1975), which has been shown to work especially well in modeling evapotranspiration in temperate climates. The two-layer UZ/ET formulation developed by Yan and Smith in 1994 is used to divide the soil into a root-uptake zone and an infiltration zone. Because the temperatures used in this analysis occur above 0°C, only evapotranspiration due to canopy interception and evaporation from the canopy, plant transpiration, and soil evaporation are considered.

In modeling the BIF green roof, it was assumed that plant roots would penetrate as deep as possible in order to obtain water. This assumption is validated by the fact that companies that install green roofs typically install a root barrier beneath the water retention and drainage mats to protect the underlying roof from damage. Thus, *RD* is directly correlated with the total depth of the planting medium. The *LAI* should change over the course of the year; although some of the species installed at the study site are evergreen, at least five of them die or are cut back during the winter. These plant growth and maintenance cycles significantly decrease the amount of plant cover. However, since the storms used during calibration of the MIKE SHE model occur during the time of year when most of the vegetation will have regenerated, this change in plant cover with growth cycle was not a concern during calibration. Additionally, *LAI* was input into FERUM as a random variable during the reliability analysis, allowing its importance to be investigated. The vegetation is assumed to be uniformly distributed across each of the four beds, with no vegetation in the intervening gravel.

3.4.2 Infiltration and subsurface flow

Although green roofs make use of natural processes to reduce runoff, they are still highly engineered structures. As a result, some simplifications were made regarding the processes governing water flow into and through the LiteTop™ media, gravel, water retention panel, and water drainage mat. The LiteTop™ media and gravel were modeled in both the unsaturated and saturated modules of MIKE SHE, since they can act within both regimes. Within the unsaturated zone, the media was discretized into 0.01 m deep cell sizes, and each medium had its own soil moisture retention curve and saturated hydraulic conductivity, as described below. Within the saturated zone, the medium was assumed to have the same vertical and horizontal hydraulic conductivity, although these parameters were distinct between the gravel and the LiteTop™. However, the specific yield ($n-\theta_r$) was considered the same for both the gravel and the LiteTop™, for the sake of modeling simplicity.

In practice, the water retention and water drainage mats are only a few mm to a few cm thick. Modeling these thicknesses in MIKE SHE could cause severe computational difficulties due the small scales required to discretize and categorize the saturated and unsaturated zones in the model. Consequently, the water retention panel and water drainage mat were modeled as a single combined layer within the unsaturated zone. This layer was one of the most significant areas for calibration, since it was modeling a highly engineered surface, which has both a high hydraulic conductivity and a fairly high specific yield. Because of the nature of water movement through the drainage mat, the mat layer was assumed to be anisotropic, and the horizontal and vertical conductivities calibrated separately.

The modeling of infiltration and flow in the unsaturated zone is governed by the Richards equation (as shown in Equation 7):

$$\frac{\delta\theta}{\delta t} = \frac{\delta}{\delta z}\left[k(\theta)\left(\frac{\delta\psi}{\delta z} + 1\right)\right] \qquad \text{Equation 7}$$

Richard's equation relates the change in soil moisture content with time ($\delta\theta/\delta t$) to the soil hydraulic conductivity (k) and the change of pressure head with depth ($\delta\psi/\delta z$). The Richards equation inputs for MIKE SHE include the saturated hydraulic conductivity of the soil and a

soil water retention curve. For this particular model, the requisite water retention curve was established using the van Genutchen approximation (1980). The van Genutchen approximation requires user input of soil suction pressure, saturated water content, and residual water content. The saturated water content and saturated hydraulic conductivity of the LiteTop™ were established from estimates given by the manufacturer. Similarly, estimates for the same parameters were obtained from available literature for gravel.

3.4.3 Drainage

The subsurface drainage module in MIKE SHE was used to simulate natural and artificial drainage systems that cannot be modeled by the typical MIKE 11 river modeling program. MIKE SHE contains two different simulation options, which can be used to solve for saturated zone flow and drainage: Preconditioned Conjugate Gradient (PCG) and Successive Over-relaxation Package (SOR). Since SOR is typically used in modeling the flow of groundwater in highly sloped terrain, such as a hillside, PCG was selected as the more appropriate model. The PCG drainage model includes options to specify drain level, routing, and a 'drainage constant', which essentially tells the program how quickly to remove water from the saturated zone with respect to height. The drainage constant is representative of the density and permeability of materials around the drainage basin. Drainage flow occurs in the layer of the saturated zone where the drain is located (in this case the water retention and drainage panel). The rate of drainage is dependent upon both the drainage constant and the height of water above the drain; the drain is treated as a linear reservoir as shown in Equation 8.

$$q = (h - Z_{drain})C_{drain} \qquad \text{Equation 8}$$

q is the flow through the drain;

h is the head in the saturated zone;

Z_{drain} is the drain elevation;

C_{drain} is the MIKE SHE drainage constant

Typically, the value of C_{drain}, the drainage constant, is on the order of $1x10^{-6}$ s^{-1} (DHI Software, 2007). In the green roof model, the calibrated value was closer to $1x10^{-2}$ s^{-1} since

the hydrograph was otherwise too stretched over time. The difference between suggested and actual drainage constants was likely due to relatively small size of the saturated zone. The small difference between the head in the saturated zone and the drainage level must be compensated by a larger drainage constant in order to maintain a reasonable drainage flow. The drain height, Z_{drain}, was defined as the lowest point in the saturated zone: -0.28 m. This selection was made to ensure that (h-Z_{drain}) was maximized, as well as to imitate the drain placement on the actual green roof.

3.5 Calibration and validation

Four storms were chosen from the 2011-2013 data cycle for use in calibration and three storms were selected for validation. The storms were chosen as a representative sample of the types of storm systems observed in central Illinois. Both localized summer convective thunderstorms (high intensity short duration) and longer frontal events (lower intensity long duration) are fairly common over the course of the year (ISWS, 2006). Using a framework similar to the one adopted by Obeid (2014), a "high intensity" storm is defined as one with over 0.0254 cm/min of precipitation, and a "long duration" storm is defined as one that lasts for over 5 hours. Two of the four calibration storms selected were high intensity short duration (HISD) with the remaining two being low intensity long duration (LILD). The validation storms include two HISD storms and one LILD storm.

3.5.1 Warm up analysis

Like many other coupled surface water-groundwater models, MIKE SHE is sensitive to initial conditions. However, the further back in time before the rainfall event the model is initiated, the less impact that the initial conditions will have on the runoff outputs from MIKE SHE that are caused by the storm event. Warm up analysis was used to establish a tradeoff between model dependence on initial conditions, and the excess computational time needed for extremely long scenario runs.

The impact of changing simulation duration on peak saturated drainage flow following the rainstorm event was studied to determine the required warm up period. The time when

the warm up period appears to be most productive is at 2.5 hours. With a 20% error factor, the estimated run time was about 3 hours.

3.5.2 Calibration

The two most important calibration parameters involved saturated hydraulic conductivity and drainage. The MIKE SHE model characterized the highly engineered systems of a green roof within a natural infiltration and flow framework. Thus, the saturated hydraulic conductivity for the water retention and drainage panel in particular was a 'catch-all' parameter, capturing the interactions of the engineered systems with the soil. The drainage constant similarly was used to parameterize the overflow drain setup on the actual green roof. Although other parameters such as the saturated hydraulic conductivity of the LiteTop™ and gravel were also used in calibration, they were less important than the saturated hydraulic conductivity and the drainage constant. Both the soil and retention panel layers were assumed to be anisotropic, with greater vertical conductivity in the soil layer, and greater horizontal conductivity in the retention panel layer.

Calibration was conducted using runoff data captured from the green roof during a specific calibration storm. In particular, the calibration focused on the following parameters affiliated with the runoff: 1) lag between peak rainfall and peak hydrograph; and 2) peak hydrograph discharge. These calibration parameters are similar to parameters selected by Obeid (2014), but were adapted in this analysis to better evaluate the rising limb of the hydrograph rather than the tail. A time series for drainage flow from each of the drains can be exported from the model. This time series was then compared to the actual observed time series from the BIF green roof using the Nash-Sutcliffe error (NSE) function (Equation 9). Another important calibration factor was the ratio between the root mean squared error and the standard deviation of the observed hydrograph (RSR) (Equation 10). According to Moriasi et al (2007), model simulations for hydrological processes can be judged effective if $NSE > 0.5$ and $RSR \leq 0.7$.

$$NSE = 1 - \frac{\sum_{t=1}^{N}(q_{t,model} - q_{t,observed})^2}{\sum_{t=1}^{N}(\mu_{observed} - q_{t,observed})^2}$$ Equation 9

$q_{t,model}$ is the modeled flow at time t;

$q_{t,observed}$ is the observed flow at time t;

$\mu_{observed}$ is the mean of the observed flows over the entire time series

$$RSR = \frac{RMSE}{STDEV} = \frac{\sqrt{\sum_{t=1}^{N}(q_{t,model} - q_{t,observed})^2}}{\sqrt{\sum_{t=1}^{N}(\mu_{observed} - q_{t,observed})^2}}$$ Equation 10

The May 20, 2012, HISD storm had an NSE of 0.83 and an RSR of 0.64, meaning that it met acceptable calibration standards. Similarly, the November 7, 2011, LILD storm had an NSE of 0.76 and an RSR of 0.66. These goodness-of-fit parameters show that the calibrated model can satisfactorily simulate both HISD and LILD storms. The calibrated parameters selected for the MIKE SHE BIF model are shown in Table 3.

Table 3. Soil and drainage parameters were used for model calibration.

Parameter	Calibrated value
$k_{LiteTop}$	0.11 m/s
k_{gravel}	0.15 m/s
k_{ret} retention layer (vertical)	0.00055 m/s
k_{ret} retention layer (horizontal)	0.00957 m/s
Drainage constant	0.015 /s
Initial head	-0.115 m

CHAPTER 4: Reliability analysis

Reliability is defined as the probability that capacity is greater than demand for a given component or system. In other words, reliability determines whether a system or module is 'in failure'. The boundary at which the capacity (C) and the demand (D) are equal is known as the limit state function (G). In mathematical form, the limit state function can be defined as a closed expression using the safety margin formulation in the form shown in Equation 11, where $\boldsymbol{x}$ are all input random variables.

$$G(\boldsymbol{x}) = C(\boldsymbol{x}) - D(\boldsymbol{x}) \qquad \text{Equation 11}$$

The failure domain is defined as the set of all points where $G(\boldsymbol{x}) \leq 0$. In the context of green roof runoff, capacity (C) can be defined as a given fraction of the peak runoff produced by a conventional roof of similar area. Demand (D) is defined by the peak runoff produced by the modeled green roof. By this definition, a green roof is 'failing' if it does not reduce peak runoff below a certain percentage threshold of the runoff peak from a similarly sized conventional roof for the same storm. Other potential metrics for green infrastructure failure can be substituted for peak runoff; the same framework presented here would remain applicable. A sketch representing the concept of reliability analysis and the failure domain in $\boldsymbol{x}$-space is shown in Figure 5.

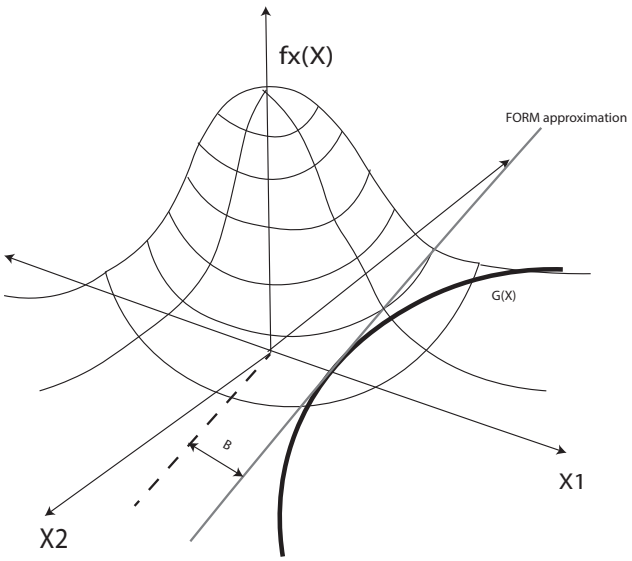

Figure 5. The FORM approximation of the limit state function *G(x)* is a linear representation of the relationship between variables.

Different methodologies are used to estimate the probability of failure (*Pf*) of a component. The first order reliability method (FORM) uses a plane tangent to ***G(u)*** at the closest point to the origin on ***G(u)*** in the standard normal space (***u***) to estimate the probability of failure. In FORM, the Hassofer Lind –Rackwitz Fiessler (HL-RF) algorithm is used to find the point on ***G(u)*** that lies closest to the origin in standard normal space. This point is known as the design point (***u****); the distance between ***u**** and the origin is known as the reliability index (β). The probability of failure (*Pf*) can then be calculated as shown in Equation 12. For more information on the HL-RF algorithm itself, see Rackwitz and Fiessler (1978).

$$Pf=\Phi(-\beta) \qquad \text{Equation 12}$$

FORM is typically a good approximation due to the properties of the standard normal space, and can be used to generate estimations of random variable importance and parameter sensitivity. However, FORM does not work for limit state functions with unusual shapes in the standard normal space. In these cases, the second order reliability method (SORM) or Monte Carlo simulations are better alternatives (Hasofer and Lind, 1974).

In this analysis, FERUM, a MATLAB-based reliability analysis engine, was used to compute the probability of failure of the BIF green roof given a certain design storm. FORM analysis was used to determine an initial estimate of *Pf*, importance, and sensitivity. SORM and Monte Carlo analysis were used to confirm estimates generated by FORM and ensure that the estimate was accurate. Design storms of different durations, return periods, and seasonality were used to create fragility curves under different peak reduction efficiencies.

4.1 Uncertainty analysis

Data taken from the green roof were analyzed to create probability distribution functions for climatic, vegetation, and soil-related properties. Table 4 itemizes the variables analyzed over the course of this analysis. The rooting depths for the plants on the green roof were assumed to be equal to the depth of the soil media, *d*. This assumption was based on the concept that tree roots will continue to grow until impeded by soil barriers, including "mechanical effects impeding root entry or survival" (Store and Kalisz, 1991). In the case of green roofs, the barrier is an artificial root stop placed below the soil media to prevent the penetration of the roots into the roof. The initial water table height (*WTH*) is a required input parameter for MIKE SHE, which can act as a substitute for initial soil water content. Thus, a high water table would imply saturated soil conditions.

Table 4. Several random variables were used to in the MIKE SHE model to complete the reliability analysis.

Random variable	Symbol	Impact on model
Total precipitation (mm)	P	Climate
Leaf area index	LAI	Vegetation
Depth of LiteTop (m)	d	Soil- unsaturated zone
Initial water table height (m)	WTH	Soil- unsaturated zone
Saturated hydraulic conductivity for LiteTop (m/s)	$k_{LiteTop}$	Soil – unsaturated zone
Saturated hydraulic conductivity for pea gravel (m/s)	k_{gravel}	Soil – unsaturated zone

Reference evapotranspiration (ET_0) was not considered a random variable during this analysis since the ET estimation was based on empirical data. An average ET_0 was estimated for the two different seasons that experience the largest amount of precipitation: 'summer' (April-July) and 'winter' (November). The two seasons were determined by analyzing the precipitation normal amounts for Urbana, Illinois; months with over 3.6 inches of precipitation and over 10 days with precipitation were selected for the analysis. An inter-storm average ET_0 was then calculated for each of these seasons using the Urbana, Illinois, climatic normal values for temperature (ISWS, 2010); monthly average wind speed for Illinois (ISWS, 2009); and monthly average relative humidity and solar radiation for Peoria, Illinois (RREDC, 1990). The normal temperature values were based on data taken from 1981-2010. Wind speed averages were based on data from 1991-2000 taken from the Illinois Climate Network. Relative humidity and solar radiation were based on data collected from 1961-1990.

Forty-five years of NOAA daily rainfall records for Central Illinois were analyzed to select the maximum annual event for each water year (NCDC, 2014). The events were ranked and the event probability characterized using Weibull ranking. A frequentist regression analysis was then conducted between the observed rainfall and model probability distribution functions (PDFs) created using the Weibull, Log Pearson III, Gumbell, and lognormal distributions. The Log Pearson III distribution was selected as the model that minimized the sum of square errors, as well as providing the closest estimation to the log sample mean and standard deviation. Figure 6 shows a linearized plot of the Log Pearson III *k* value against the log of the observed precipitation. Once the total amount of precipitation for each design storm was calculated, triangular hyetographs were generated for 2-hour and 24-hour duration storms following the methodology described by Yen and Chow (1980).

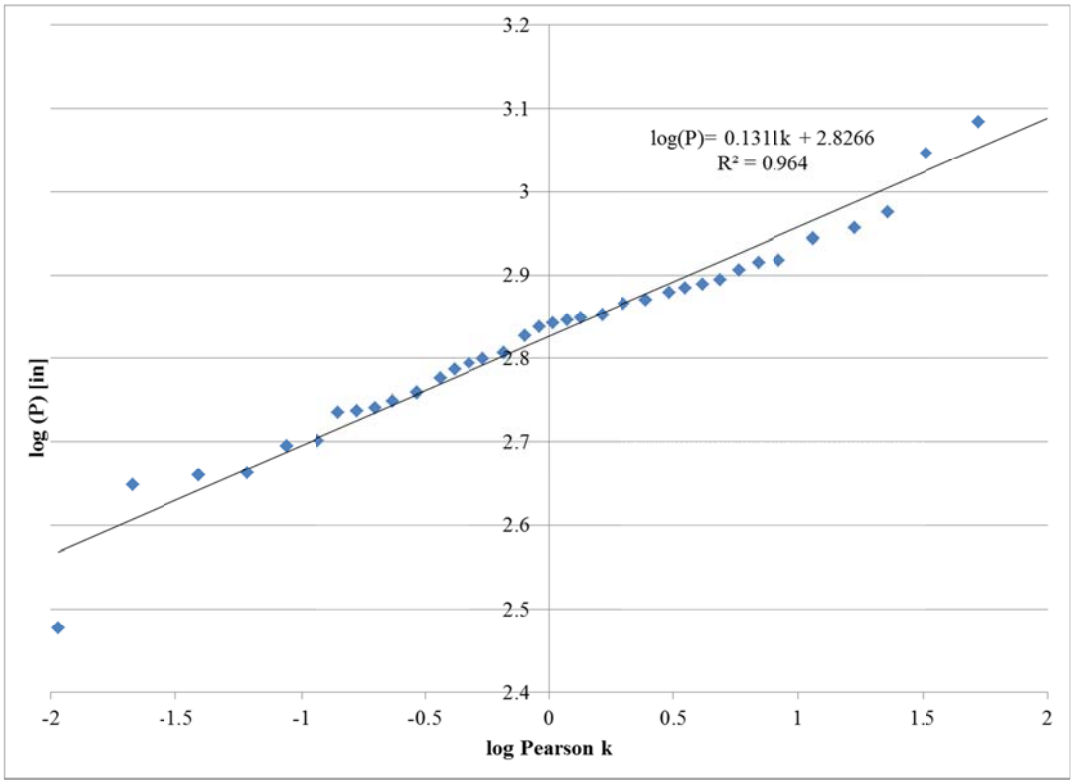

Figure 6. The linearized plot showing log Pearson III *k* value versus log precipitation reveals a suitable fit.

A similar procedure was used in determining the PDFs for the LAI vegetation parameters. Data from the Oak Ridge National Laboratory (ORNL) global leaf area index

suggest an average LAI for grasslands of 1.98 with a standard deviation of 1.46 (ORNL, 2000). Data were taken from 28 different sites, and the standard deviation of the sample mean and variance taken using the frequentist approach. The best fit distribution was a gamma distribution with parameters α of 1.71 and β of 1.06. Figure 7 shows a plot of the cumulative distribution of observed and calculated LAI.

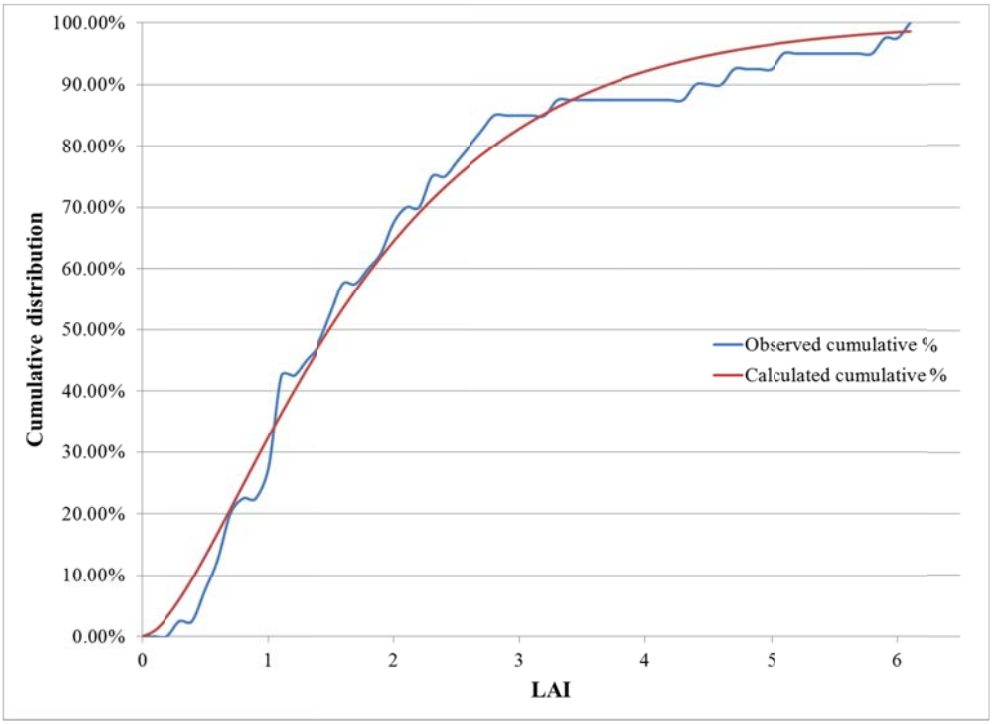

Figure 7. Observed and calculated values of the cumulative distribution of LAI show close agreement.

Very little data exist for variables relating to the soil properties other than the mean values provided by the LiteTop™ manufacturer. Engineering judgment was used to assume upper bounds for the variables, and the standard deviation derived by taking the difference between the mean and the upper bound and dividing by three. The number of samples (n) taken in determining the mean was assumed to be very large, since the product is designed by a large-scale manufacturing firm (American Hydrotech, Inc.). Hence, using the frequentist approach, the relationship $\sigma_M=\sigma/\sqrt{n}$ holds, such that σ_M can be approximated as very small. The frequentist approach was used instead of maximum likelihood estimation or Bayesian inference due to the lack of data outside the parameters provided by the manufacturer.

Finding the variance of the standard deviation is slightly more challenging, since the frequentist estimation of variance of the unbiased sample variance (Var[s^2]) is related to the fourth central moment of the distribution, μ_4. The equations used to estimate Var[s^2] and μ_4 for the different distributions used in the model are stated in Equation 13. Once again, the *n*-value in the denominator leads to a very small variance as the number of samples becomes large. Table 5 summarizes the mean, standard deviation, standard deviation of the sample mean, variance of the sample variance, and distribution type for each of the random variables.

$$Var[s^2] = \frac{1}{n}[\mu_4 - \mu_2^2 \frac{n-3}{n-1}] \quad \text{Equation 13(a).General form}$$

$$Var[s^2] = \frac{2\sigma^4}{n-1} \quad \text{Equation 13(b). Normal form}$$

$$\mu_4 = e^{4M+2Var}(e^{Var}-1)^2(e^{4Var}+2e^{3Var}+3e^{2Var}-3) \quad \text{Equation 13(c). Lognormal form}$$

$$\mu_4 = 3k^2 + 6k \quad \text{Equation 13(d). Gamma form}$$

Table 5. Different random variable distributions and sample distribution variance values were used to complete the reliability analysis.

Variable	μ	σ_M	σ	**Var[s^2]**	**Distribution type**
LAI	1.90	0.56	1.46	0.09	Gamma
d	0.2	0.001	0.017	0.001	Lognormal
WTH	0.15	0.003	0.01	0.003	Lognormal
$k_{LiteTop}$	0.0011	$3x10^{-6}$	0.00003	$3x10^{-6}$	Lognormal
k_{gravel}	0.15	$6x10^{-5}$	0.05	$6x10^{-5}$	Lognormal

4.2 Generating the capacity and demand functions (*C* and *D*)

The capacity function (*C*) was created using the MIKE SHE land surface and overland flow features to simulate impervious cover (effectively paving) throughout the entire modeled surface except for the drain locations. Runoff observed from the actual conventional roof was then scaled up to match the size of the green roof, and used to calibrate the impervious (paved) conventional roof model. Peak runoff values from the conventional roof model were then measured for each of the design storms. Figure 8 illustrates the peak runoff values for 2-hour duration storms of different return periods for the conventional roof model.

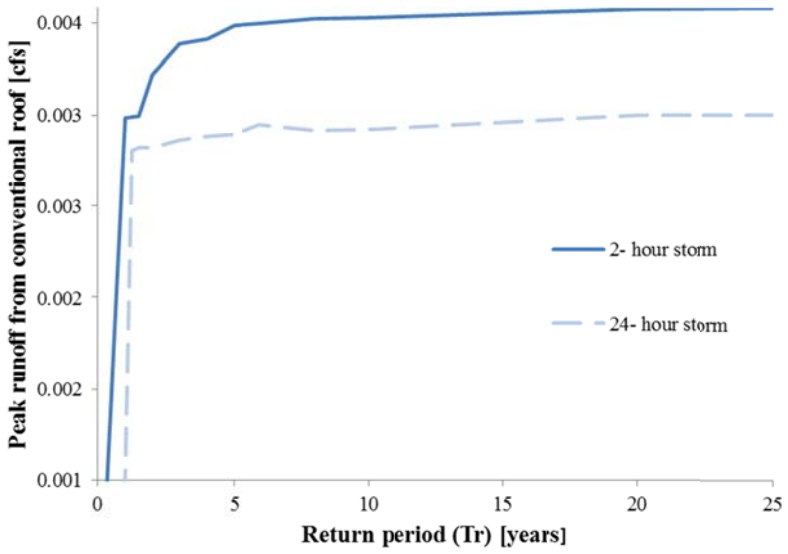

Figure 8. Peak runoff from the convention roof model varies for the 2-hour and 24-hour storms.

Hydrograph outputs from the MIKE SHE green roof model were used to generate the demand function (*D*). Twenty-six different runs were conducted for each of the design storms, using different variable parameters. Regression analysis was then used to create a synthetic demand model that could be input directly into the limit state function used in FERUM. The demand model was set up in the form shown in Equation 14. The sum of square errors for the twenty-six runs was minimized to determine the value of each of the

parameters C_i. The mean and standard deviation of the optimized model parameters could then be calculated using the data from the 26 runs.

$$D_{modeled}{}^{x} = C_0 + C_1(LAI)^x + C_2\left(\frac{d + 0.08 - WTH}{d}\right)^x + C_3\left(\frac{k_{lite}}{k_{gravel}}\right)^x + \sigma\varepsilon \qquad \text{Equation 14}$$

Box-Cox transformations have been widely adopted as one of the standard simplest and most functional transformations to remove heteroscedasticity from a regression model (Sakia, 1992). In order to conserve the homoscedasticity of the model error parameter σ, different Box-Cox transformations were tested by varying the value of x from -2 to 2. The transformation ln(D) was used instead of x=0. The heteroscedasticity of σ was tested using both a visual check and the Spearman rank correlation test. The value of σ was calculated using Equation 15; the value of x was chosen to minimize σ whilst preserving a constant σ for all values of D.

$$\sigma = \sqrt{\frac{(sum\ of\ square\ errors)}{n}} \qquad \text{Equation 15}$$

As mentioned previously, the calculation of the HL-RF reliability index β is a pre-requisite for the calculation of the probability of failure, such that $Pf = \Phi(-\beta)$. For this analysis, the calculated value of β was made using a frequentist point estimate for the mean of the model parameters as shown in Equation 16 (a). The error bounds of the probability of failure can be constructed by estimating the variance of β in terms of the parameters as shown in Equation 16 (b), where $\Sigma_{\theta\theta}$ is the covariance matrix of the model parameters, and $\nabla_\theta\beta$ is the gradient of the reliability index with respect to the model parameters (in other words, the sensitivity). Defining the bounds on β as $E[\beta(\theta)] \pm \sqrt{Var[\beta(\theta)]}$ gives an 86% confidence interval in the value of β.

$$E[\beta(\theta)] \approx \beta(\mu_\theta) \qquad \text{Equation 16 (a)}$$

$$Var[\beta(\theta)] \approx \nabla^T{}_\theta\beta\Sigma_{\theta\theta}\nabla_\theta\beta \qquad \text{Equation 16 (b)}$$

CHAPTER 5: Results

5.1 Fragility curves

Failure in the context of this analysis is defined as the inability of a green roof to reduce peak runoff below a certain standard. This standard is defined as a percentage reduction from the peak runoff measured from a similar conventional roof under the same storm conditions. Reliability analysis was conducted using the MATLAB-based software FERUM, and used to compare fragility curves created from both 2-hour and 24-hour duration storms. Figures 9 and 10 show the fragility curves from the 2-hour and 24-hour duration storms respectively. The four different curves show different standards of reduction, with the >0% reduction being the lowest standard, and the >90% reduction being the highest standard. The >0% reduction standard represents any peak runoff reduction from a green roof, while the >90% reduction standard requires that the green roof reduce peak runoff by at least 90%. The shaded areas depict the 86% confidence interval for each curve, based on the reliability analysis described in Chapter 4. As expected, the lower green roof performance standards typically show lower probabilities of failure than the higher standards. In addition, higher return period storms (representing lower probabilities of occurrence in any given year) typically show higher probabilities of failure for the same peak reduction standard.

During the sensitivity analysis, evapotranspiration variables were shown to be more important for the long duration storm than for the short duration storm. Consequently, fragility curves were also created for long duration winter storms, since evapotranspiration is much lower in the winter season. Fragility curves were produced using winter evapotranspiration data, as described in Section 4.1. In addition, because the majority of the plants on the green roof go dormant, are cut back, or die during the winter, the LAI and RD for the MIKE SHE model were reduced to zero. Figure 11 shows the fragility curves from the winter storms.

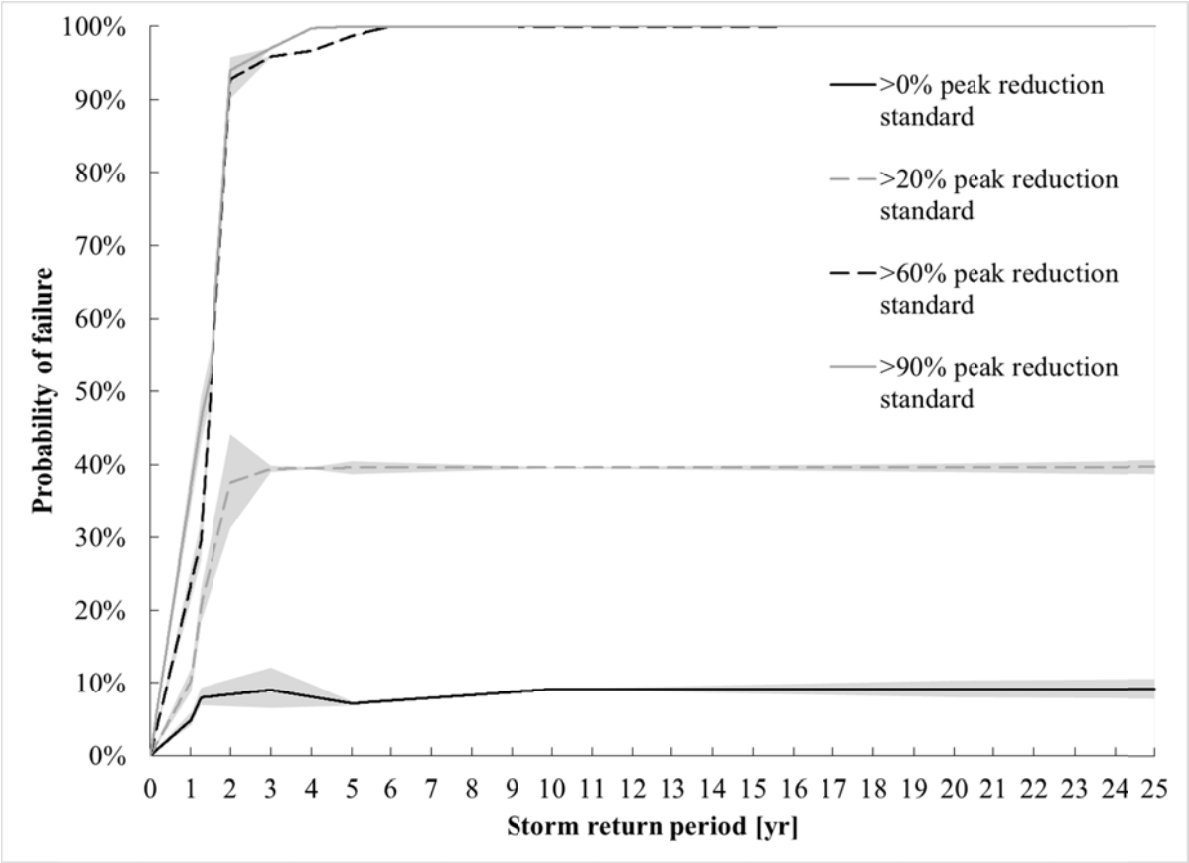

Figure 9. Fragility curves for different standards of reduction for summer 2-hour duration storms show different behavior based on peak reduction standard, with green roof performance dominated by infiltration processes.

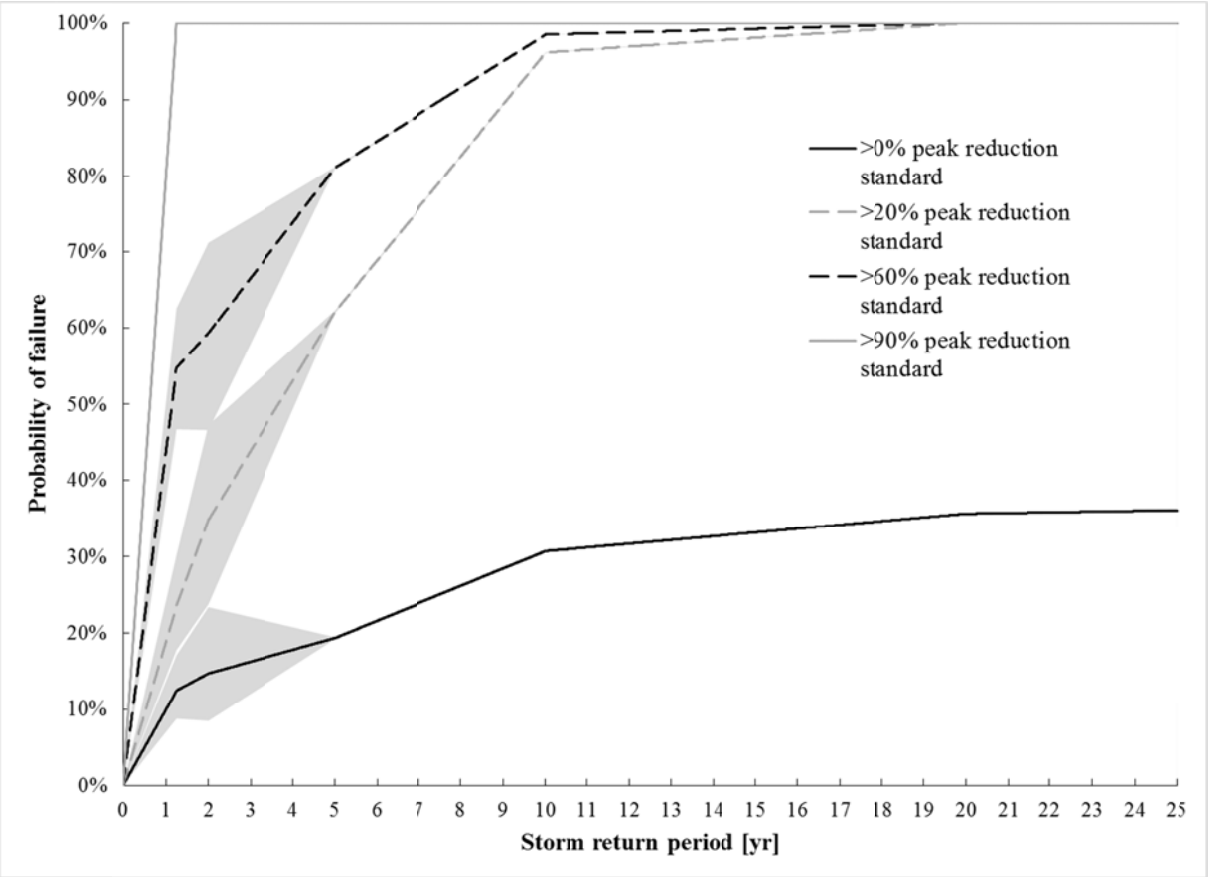

Figure 10. Fragility curves for different standards of reduction for summer 24-hour duration storms show different behavior based on peak reduction standard, with green roof performance dominated by evapotranspiration and saturation processes at low return periods.

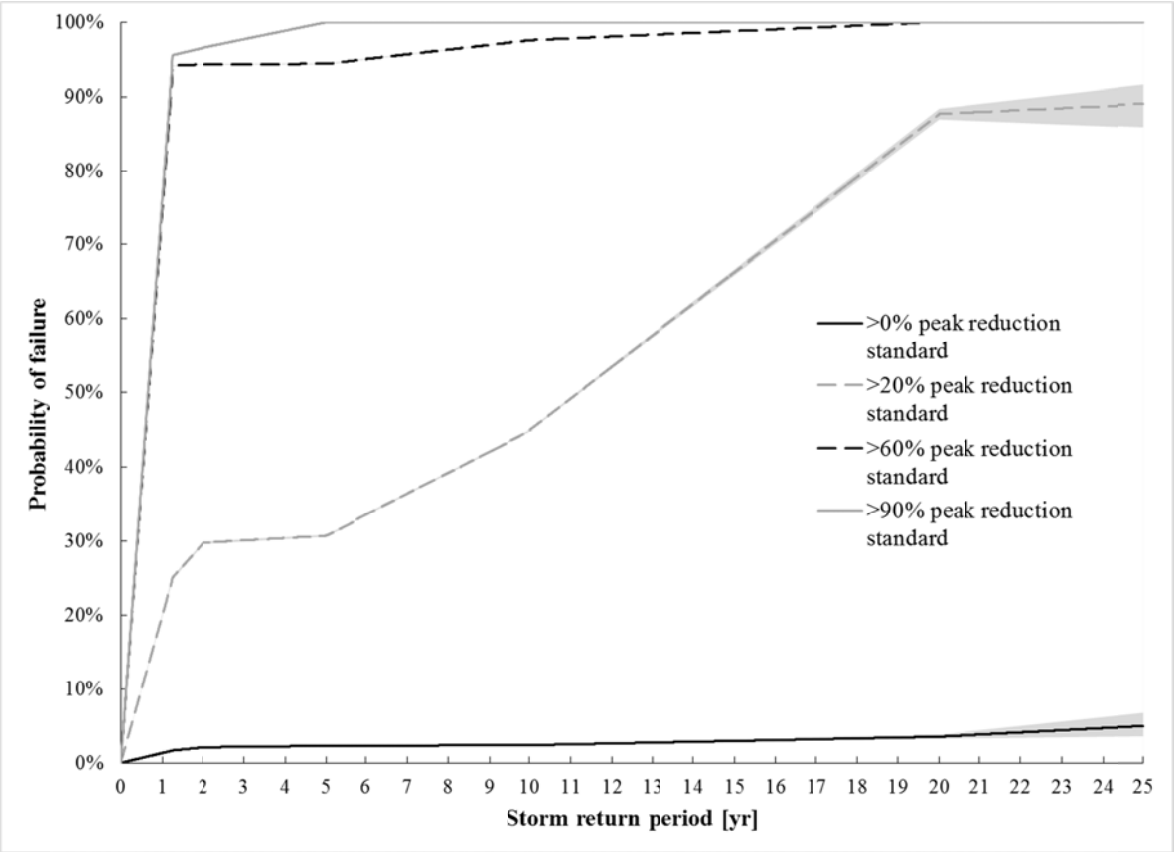

Figure 11. Fragility curves for different standards of reduction for winter 24-hour duration storms show different behavior based on peak reduction standard, with green roof performance dominated by a combination of different processes.

Some important features can be observed from the short duration storm fragility curves. The probability that this green roof will show some improvement over a conventional roof is quite high, especially for storms with low return periods. For instance, a 1-year storm with a 2-hour duration has a 5% probability of failure at the lowest standard of reduction (>0% reduction). Even for storms with a high return period, there is a high probability that the green roof will at least slightly decrease the runoff peak; the probability of failure remains relatively constant at around 10%. If the standard is increased even slightly, to 20% or greater peak reduction, the probability of failure increases dramatically. The probability of failure for the 1-year storm doubles to 10%, and the probability of failure of the 25-year storm is almost 40%. In other words, for the larger (lower probability) storm event, around

one in two events will fail to meet the runoff reduction criterion. In the case of the 2-hour duration storms, although the probability of failure remains consistently low for the 1-year, 1.25-year and 1.5-year storms, it spikes dramatically by the 2-year return period storm. This rapid increase in the probability of failure indicates that for short duration storms, green roofs are most effective at reducing runoff for storms that have a less than a 2-year return period (i.e., more than 50% chance of occurring any given year).

Comparing the 2-hour and 24-hour fragility curves in Figures 9 and 10, respectively, the green roof is most likely to fail for the long duration storms under the current criteria for low return period events. This modeled failure is likely because the capacities (a given fraction of the peak runoff produced by a conventional roof of similar area) for the 24-hour storms are much lower than the 2-hour storms. Hence, the likelihood that the demand will equal the capacity for the 24-hour storms is higher. The mechanisms that produce runoff in both cases might also be responsible: runoff in the short duration storm is infiltration dominated, but runoff in the long duration storm is mostly saturation dominated. The shape of the fragility curves for the 24-hour storms is much flatter sloped than the fragility curves for the 2-hour storms. In other words, there is no consistently sharp inflection point in the probability of failure when comparing short duration and long duration storms. However, there is a clear increase in the uncertainty associated with the probability of failure around the 2-year return period storm. While a similar increase can be observed in both sets of fragility curves, the increase in uncertainty is less pronounced in the 2-hour (short duration) storms than in the 24-hour (long duration) storms.

The high amount of uncertainty in the probability of failure is concentrated in the low return periods of the curves for both storm durations, and decreases dramatically as the fragility curves approach 100%. This trend in uncertainty implies that the point at which the green roof becomes completely impractical for different storms can be identified easily. For instance, a green roof undergoing a 2-hour duration storm will almost always fail (probability of failure >99%) to meet the 60% reduction standard by the 6-year return period event. In contrast, a green roof undergoing a 24-hour duration storm will almost always fail to meet the 60% reduction standard at the 20-year event. In other words, the probability of failure for the lower return period storms is higher for the 24-hour (long duration) storm, but the

probability of failure is lower during long duration storms for the higher return period storms. This shift in the relative probabilities of failure is due to the relative steepness of the two sets of fragility curves: while the 2-hour duration curves initially display low probabilities of failure, the probabilities increase steeply towards an asymptotic value. Interestingly, the probability of failure for the green roof is typically lower for the longer duration storm curves than it is for the shorter duration storms, but only for the higher standards.

The long duration winter storm curves show many similarities to the short duration summer storm curves. The highest standard curves show a similar shape to the curves for the short duration summer storms, with a rapid increase to an asymptotic value. However, the two lower standards show much slower rates of increase, similar to those associated with the summer long duration storm curves. The winter storms typically have lower probabilities of failure than the long duration summer storms. For the most part, the uncertainty in the probability of failure for the winter storms is much smaller than for most of the other storms, although the uncertainty does increase for larger storm return periods.

As expected, green roofs behave differently under different storm scenarios. In general, the best performance is observed for low duration, low return period storms as compared with higher return period storms. However, green roofs perform better in higher return period storms if they are of longer duration. These observations are consistent with findings in existing literature (Carter and Rasmussen, 2006; Davis, 2008), but expand on previously published results to reveal more quantitative information about peak runoff reduction performance.

5.2 Comparing results from FORM, SORM and Monte Carlo

In general, results of reliability analysis for FORM, SORM, and Monte Carlo analysis are fairly consistent across storms. The one notable exception to this rule occurs in the case of the 2-year return period storms for both long and short duration summer storms. In both cases, the 2-year storm is one of the few non-linear regression fits used to describe the MIKE SHE outputs. As discussed in Section 4.2, a Box-Cox transformation was used to reduce the heteroscedasticity of the fit where needed. However, for the 2-year storm, this transformation

produces a mismatch between the Monte Carlo simulation results and those produced by FORM. This inconsistency indicates that the linear approximation used by FORM is not a good fit for calculating the probability of failure within this probability space for expressions of the form used to describe the 2-year storm. This poor fit might be due to the curvature of the limit state function $G(\boldsymbol{x})$ at the design point. However, FORM provides an accurate result for most storms, indicating that the importance and sensitivity analysis produced for this model are dependable.

5.3 Importance and sensitivity analysis

Importance and sensitivity analyses provide important insights into the mechanisms that have the largest impact on peak runoff reduction. Importance analysis focuses on the effect that the random variables themselves have on β, whereas sensitivity analysis quantifies the impact of distribution parameters (such as μ and σ) and model parameters (the multipliers and constants in the demand regression model, and the capacity, C). Mathematically, importance can be expressed as $\nabla_{u*}\beta$, whereas sensitivity can be expressed as $\nabla_{\theta f}\beta$ for distribution parameters and $\nabla_{\theta g}\beta$ for model parameters. To ensure that the sensitivities are comparing meaningful changes rather than 'unit' changes, the distribution parameter sensitivity matrices must then be multiplied by the standard deviation of the variables. The resulting vectors are known as $\boldsymbol{\delta}$ when used to describe the sensitivity of β to the means, and $\boldsymbol{\eta}$ when used to describe the sensitivity of β to the standard deviations (Gardoni, 2014).

Observing the difference in sensitivities and importance vectors for low versus high return periods and long versus short duration storms reveals interesting conclusions. To ensure that the sensitivity analyses provided by FORM were accurate, storms were chosen for each of these categories that minimized the difference in results between the outputs for FORM and Monte Carlo. The four summer storms, which were chosen as representative for sensitivity analyses, were: 1) the 1-year 2-hour storm, 2) the 20-year 2-hour storm, 3) the 1.25-year 2-hour storm, and 4) the 25-year 2-hour storm. Figure 12 summarizes the importance analysis results for the four different categories of storms.

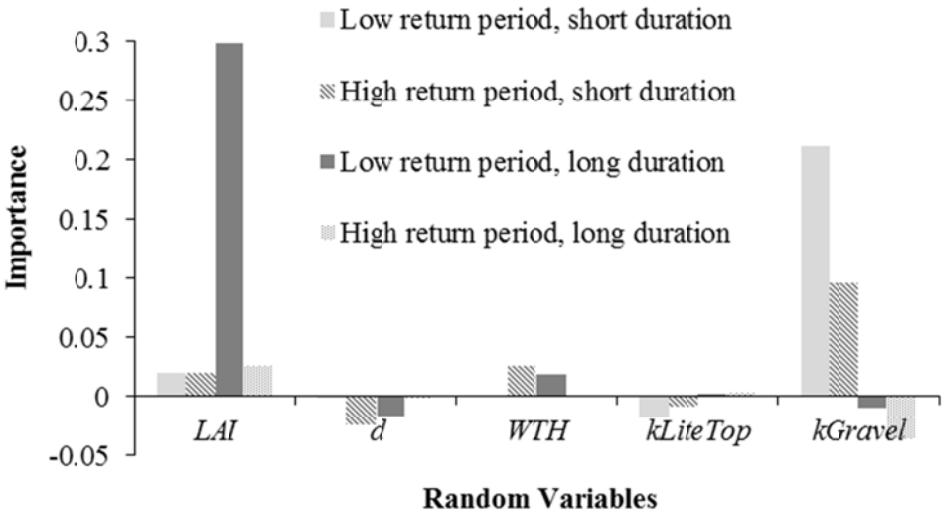

Figure 12. The importance analysis of variables for different types of summer storms reveals varying levels of importance for random variables of leaf area index (*LAI*), planting medium depth (*d*), water table height (*WTH*), LiteTop hydraulic conductivity ($k_{LiteTop}$), and gravel hydraulic conductivity (k_{Gravel}).

In the case of the low return period, low duration storm, k_{gravel} is the most important variable. The importance of the two saturated hydraulic conductivities was not equal; $k_{LiteTop}$ is approximately one tenth as important (on the same order of magnitude as the importance of the *LAI*). The mean of k_{gravel} is also the most sensitive distribution parameter. Interestingly, the sensitivity of $k_{LiteTop}$ is negative, signifying that it is a 'demand variable': increasing this parameter increases the probability of failure, *Pf*. This finding makes physical sense when the design of the green roof is considered: higher hydraulic conductivities allow water to flow rapidly through the media and into the drain. In other words, the green roof in this case begins to act increasingly more like a conventional roof in terms of the runoff. Table 6 shows the sensitivity of the probability of failure to the model parameters described in Section 4.2. The capacity value is the most sensitive among the model parameters. It dominates the other parameter sensitivities by almost two orders of magnitude, highlighting the importance of a well-defined capacity function in determining the probability of failure.

Table 6. The probability of failure is highly sensitive to some of the model parameters.

Model parameter	Sensitivity for 1.25-year, 2-hr storm
Capacity	-41.4
C_0	0.14
C_1	0.07
C_2	-0.11
C_3	0.09

A high return period, short duration storm follows many of the same characteristics. Infiltration parameters still dominate, and capacity still plays a major role in determining the probability of failure. However, the relative importance of each respective parameter is more evenly distributed, showing that saturation variables such as *WTH* and *d* do play a significant role in failure. The overall sensitivities are also higher in general; most interestingly, the values of $\boldsymbol{\eta}$ are typically much larger, showing that the standard deviations of the distribution parameters become increasingly important for modeling larger storm events.

A different pattern emerges when the same analysis is applied to the long duration storms. For the low return period, long duration storm, the importance of the evapotranspiration variable *LAI* becomes predominant, with the importance of the saturation variables *WTH* and *d* following close behind. The distribution mean sensitivities ($\boldsymbol{\delta}$) follow a similar trend. The distribution standard deviation sensitivities ($\boldsymbol{\eta}$) values are around one order of magnitude less than the values of $\boldsymbol{\delta}$. In general, the model parameter sensitivities are higher than the sensitivities for the shorter duration storms. However, the capacity value is no longer the most sensitive parameter; many other model parameters are on the same order of magnitude in terms of sensitivity. High return period, long duration storms once again have a much higher importance for infiltration variables, but also have high, evenly distributed model parameter sensitivities. Similar to the short duration storms, model parameter

sensitivity increases for high versus low return period storms. However, the distribution parameter sensitivities decrease.

Comparing the long duration winter storm to the long duration summer storm also yields interesting results. Figure 13 compares the importance of different variables for the winter and summer storms. The importance of saturation variables is much higher for the low return period winter storm than it is for the corresponding summer storm. However, the saturated hydraulic conductivity, particularly k_{gravel}, plays an important role as well. Without the presence of plants to help redistribute the water within the planting medium, both saturation and infiltration are equally important for reducing peak runoff. The winter high return period storm is, however, mostly infiltration dominated, similar to its summer counterpart. Interestingly, the parameter sensitivities decrease by several orders of magnitude between the low return period winter storm and the high return period winter storm.

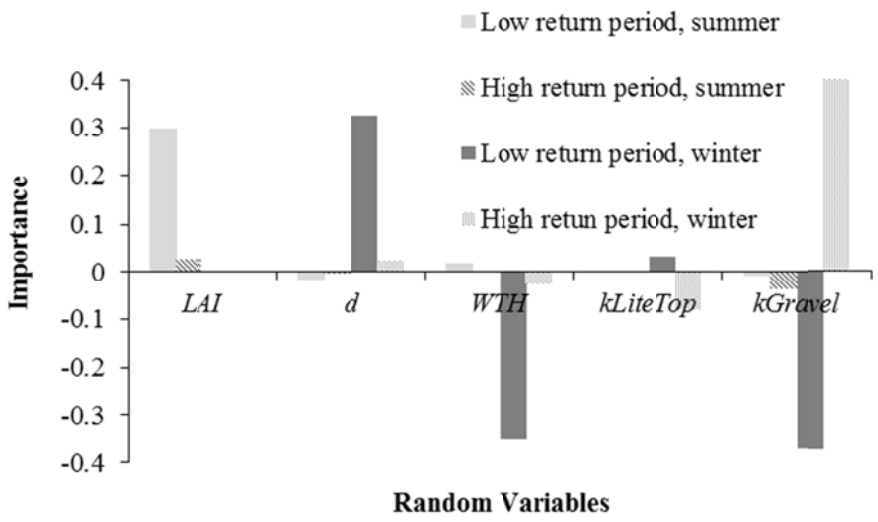

Figure 13. The importance analysis of variables for winter and summer storms reveals varying levels of importance for random variables of leaf area index (*LAI*), planting medium depth (*d*), water table height (*WTH*), LiteTop hydraulic conductivity ($k_{LiteTop}$), and gravel hydraulic conductivity (k_{Gravel}).

The sensitivity and importance analyses reveal important differences in the mechanisms that control green roof runoff. While the short duration summer storms are infiltration-

dominated, the long duration storms are controlled by a variety of different factors. The evapotranspiration variable *LAI* plays a major role during the low return period, long duration summer storms; it is absent from the winter storms because of plant dormancy. However, saturation variables do play an important role in both winter and summer long duration storms as well. Saturation and infiltration mechanisms are both equally important during low return period winter storms. In all cases, high return period storms are infiltration-dominated.

CHAPTER 6: Policy implications

Green roofs have multiple benefits beyond the reduction of stormwater runoff and improvements in local water quality. Green roofs can help to regulate the urban heat island effect, reducing air quality issues such as smog, decreasing the amount of energy needed to cool buildings in urban areas, and improving the overall quality of life (Virk et al, 2015). Studies show that the presence of green infrastructure in urban environments can improve physical and mental health, and have even been correlated with reductions in local crime (Kondo et al., 2015). Green roofs can also have multiple economic benefits. Multiple studies have shown that green roofs can help to reduce building energy consumption by helping to regulate internal temperatures (Niachou, 2001). The extra vegetative cover also helps to extend the lifetime of roofing materials by providing protection from physical and UV damage (Niachou, 2001). Indeed, life cycle analysis studies of green roofs have shown that although the upfront costs of green roofs are greater than those of traditional roofs, green roofs often pay for themselves over time (Wang et al., 2013).

Despite all of these economic, environmental and social benefits, green roofs still struggle with barriers to implementation related to their perceived risk and upfront costs. For the most part, green roof implementation in the United States still suffers from knowledge gaps between green roof experts and building owners and occupants actually making use of the roof. There is a general lack of consistent information quantifying the performance, costs, and benefits of green roofs, which has led to the perception of green roofs as risky investments. This perception is further exacerbated by the fact that green roofs generally have higher upfront and maintenance costs than conventional roofs. The parties in charge of building and maintaining green roofs are typically not the people who benefit from the green roof installation. This phenomenon has created a disconnect between green roof planning and implementation. Finally, regulatory and fiscal policy at the state, federal, and local level can be incompatible with the installation of green infrastructure (Malina, 2011). For instance, Louisiana's Administrative Code forbids the creation of wet basins or other ponded areas that might cause an influx of disease vectors such as mosquitoes. However, the draft critical

zoning ordinance calls for the use of retention basins and wetlands to help reduce local flooding in the New Orleans area (Sonne, 2014).

Cities have developed innovative new incentives to try to overcome these barriers. Germany, the current world leader in green roof implementation, is also historically the oldest consistent proponent of green roofs. Although investments in local sewer systems have been fairly consistent, Germany still faces issues with flooding in urban areas due to increased urban population and storm intensity. Germany has used a variety of different approaches to incentivize municipalities and private developers to actively consider green roofs as an option for stormwater reduction. As of 2003, almost one-third of all municipalities within the country had stormwater policy instruments in place to promote green infrastructure. Of the municipalities surveyed, nearly half provided indirect financial subsidies for green infrastructure implementation, while one-third had municipal regulations mandating the use of LIDs for stormwater management. The remaining municipalities provided direct financial subsidies for green infrastructure implementation. Many cities, such as Berlin, also opted to create pilot projects to combat initial skepticism, and have incorporated green infrastructure into a multi-benefit system of spatial planning and zoning ordinances (Nikel et al., 2014).

These municipal efforts are bolstered by a network of national and regional laws that address the same issue. After 2008, the German Wasserhaushaltsgestz (Water Act) has prioritized solutions that infiltrate stormwater near its source. As a part of this prioritization, developments that include green infrastructure are allowed an expedited permitting process, and no longer need permission to infiltrate lightly polluted stormwater. German case law also calls for separate stormwater fees based upon estimates of actual contribution of the parcel of land to the total stormwater burden. The fees are then discounted for areas containing LIDs, and are considered an efficient form of incentive for local landowners. On a broader scale, Germany's initiatives fall under the European Water Framework Directive (EWFD), which was implemented in 2000. The EWFD sets limits on both emissions and water quality standards for rivers and streams within the European Union, similar to the system of total maximum daily loads employed by the U.S. Environmental Protection Agency (USEPA) (Nikel et al., 2014).

Within the United States, similar initiatives have been adopted by cities across the country, with varying degrees of effectiveness. Indirect financial incentives are by far the most popular. New York City's green infrastructure implementation plan (PlaNYC) includes tax abatements for buildings with green infrastructure. The use of tax abatements provides developers an easy metric to include in economic assessments and evaluate immediate and long-term benefits (Jones, 2009). Portland plans to use financial incentives tied to zoning ordinances to encourage the use of green infrastructure in certain parts of the city (Malina, 2011). Green infrastructure programs in Chicago and Indianapolis feature expedited permitting for developers who make use of green infrastructure in their designs (Malina, 2011; Sonne, 2014). Finally, many cities in states such as Maryland have chosen to add stormwater remediation fees. The fee rates are typically proportional to the impervious area in each lot, and go towards maintaining the stormwater utility and restoring and protecting the local watershed. Fee discounts are available for lots that make use of green infrastructure. While these fees have been shown to be effective, they need to be high enough to incentivize action, and should ideally take into account geographic discrepancies that have an effect on local stormwater drainage (Sonne, 2014). While direct financial incentives, such as Chicago's private sector Green Roof Grant program, remain in use, they are generally not viewed as financially sustainable in the long-term (Malina, 2011).

An alternative approach is to use municipalities' regulatory power to enforce performance or technology standards. Performance standards give developers the flexibility to choose whether or not to use green infrastructure to meet certain mandatory requirements for new buildings. For instance, the Chicago Energy Code has minimum solar reflectivity requirements, which all new development must meet, partly in order to reduce the urban heat island effect. Many developers choose to meet the requirements by installing green roofs on their buildings, but they are not required to do so. Similarly, both Portland and Toronto have stormwater management requirements. However, Toronto goes one step further: additional mandates are in place that require all buildings of a certain type to have green roofs, making Toronto the leader in green roof regulation in North America (Malina, 2011).

Whether cities choose to use incentives or regulation, they often still face implementation challenges. Because of the lack of information on green infrastructure

performance, mandatory standards run the risk of being either too strict or not strict enough. Similarly, because incentives are voluntary and investor driven, developers might choose not to install green infrastructure due to uncertainty about quantifiable costs and benefits (Malina, 2011). Even when cities have worked to create tools that can help developers better understand and choose appropriate forms of green infrastructure, the tools are often incomplete. The Bayou Land Resource Conservation and Development Council (Bayou Land RC&D) has worked with the city of New Orleans to create a set of tools that can be used to evaluate and choose BMPs for different water quality and runoff criterion. However, the tools use a single design storm to create the performance standards (Sonne, 2014). Because green infrastructure performance is so reliant on storm intensity and duration, as demonstrated by this reliability analysis, the tools might not be able to properly evaluate the suitability of green infrastructure for a given area.

The use of fragility curves can help municipalities and developers better understand in which context green infrastructure is a good fit. Moreover, they provide a set of criteria to help evaluate whether or not green infrastructure is still working as promised once it is installed. The simultaneously generated sensitivity and importance analyses also provide a reasonable understanding of potential areas for improvement. Within a systems-level context, fragility curves can help city planners evaluate areas that might be at risk from flooding, CSOs, or other adverse effects during certain types of storms. The incorporation of fragility curves into tools used to incentivize the implementation of green infrastructure helps to reduce its perceived risk by providing more open access to performance information for different storms. Overall, fragility curves provide a methodology for the long-term evaluation of green infrastructure within a given context, and can help developers and planners to better decide where it will be most effective.

Outside of municipal regulation, developers are also often incentivized to implement green infrastructure by outside certification schemes such as Leadership in Energy and Environmental Design (LEED) certification program. The organization that promotes LEED (U.S. Green Building Council) acknowledges that understanding performance, materials, and types of best management practices (BMPs) change over time, and so have consistently made efforts to ensure that LEED is adaptable and updated regularly. However, the constantly

changing standards have created a sort of 'moving target' for investors. This lack of consistency means that the 'value' of a sustainable property might not be stable if the market perceives risks or uncertainty in the rating system that was used to evaluate it (DeLisle et al., 2013). The use of fragility curves for green infrastructure can help to mitigate some of these perceptions of risk by helping developers and buyers better understand the strengths and limitations of particular types of green infrastructure. Developers can then better choose options that are most cost effective for them to reach the LEED classification standard that they desire.

Within the United States, most of the leading initiatives in on-the-ground implementation of green infrastructures have taken place at the city level. However, there are some actions being taken at the federal level to encourage the implementation of green infrastructure at a national scale. Like most water quality provisions, stormwater management falls under the jurisdiction of the Clean Water Act (CWA), which was enacted in 1977 and later amended in 1987. A system of National Pollutant Discharge Elimination System (NPDES) permits are in place for point discharges, such as those from storm and sewer pipes. Perhaps more crucial for stormwater management, the USEPA has implemented a series of Phase I and Phase II rules, which require municipal separate storm systems (MS4s) to achieve a set of stormwater management objectives. They are encouraged to do so using BMPs and LIDs as often as possible. For combined sewersheds, the USEPA has suggested an Integrated Framework in which the USEPA would work together with municipalities to fully consider their combined CWA obligations without focusing on each individual CWA requirement. The Integrated Framework is designed to allow for NPDES requirements for both combined and separated sewer systems, while building in flexibility in the ways that cities can meet their water quality goals (Holloway et al., 2014).

However, the USEPA's current approach to managing stormwater is mainly through consent decrees. The consent decrees are typically rigid, time-bound, and decrease the flexibility of municipalities to weigh different options for cost-effectiveness. These consent decrees are typically also highly disjointed from local initiatives, and are divorced from local conditions and community involvement, which can greatly facilitate or hinder the roll-out of green infrastructure implementation. Many cities struggle to finance the requirements

mandated by top-down driven consent decrees, which do not usually come with federal funding. In other words, the USEPA currently treats municipal governments as "polluters not partners" (Holloway et al., 2014). An alternative approach, suggested by Freeman and Farber (2005), would be a modular approach to environmental regulation, which would be based on agreement between the local and federal governments rather than command and control. This modular approach would be multi-stakeholder and locally tailored, rather than the "one-size-fits-all" approach currently encouraged by the consent decrees. Within this approach, the use of fragility curves could enable better communication between local and federal governments, by encouraging an understanding of when the implementation of green infrastructure would be most effective in terms of quantified performance.

CHAPTER 7: Conclusion

Green infrastructure is becoming an increasingly attractive alternative form of stormwater management within urban environments. A multi-benefit solution for many of the problems facing modern cities, green infrastructure has often been touted as a 'silver bullet' for urban failings. In particular, green roofs are highly valued by urban planners because of their apparent environmental, economic, and social sustainability, as well as the fact that they take up very little additional space. However, few standards exist that adequately define when green roofs are functioning as expected. Like many forms of green infrastructure, the ability of green roofs to reduce runoff is contingent on a variety of different factors. Climatic factors such as storm intensity and duration have been shown to have a particularly large impact on green roof performance. Green roof design standards currently do not capture the time varying aspect of green roof performance. This omission makes accurately evaluating green roof performance challenging.

The analysis provided in this document provides a quantifiable approach to green roof evaluation, answering the motivating question:

How might we quantify the efficiency in peak runoff reduction of green roofs?

The approach is based on a reliability analysis graphical technique known as fragility curves. Fragility curves show the probability of failure of a system or module for different standards of performance at different levels of intensity. While this approach has been consistently used in multiple fields, including earthquake engineering, this analysis is the first, to the author's knowledge, to apply it to green infrastructure. In this approach, failure was considered to be the inability of a green roof to reduce runoff below a certain standard. Two sets of fragility curves were created for summer 2-hour and 24-hour storms, covering return periods of up to 25 years, with additional fragility curves characterizing long duration winter storms. The 'standards' used to generate the curves were based on different percentages of runoff reduction from the runoff peak produced by a conventional roof. To create the fragility curves, a coupled surface-water groundwater model was used to simulate the impact of storm events of different intensities and durations on a green roof located on

the University of Illinois at Urbana-Champaign campus. The runoff hydrographs generated were subjected to a regression analysis to produced algebraic expressions of peak runoff as a factor of different variables related to vegetation and soil parameters. These expressions were then used to calculate a probability of failure using reliability analysis software.

As expected, different storms of different durations and intensities had different behaviors. In general, the green roof performed well under low intensity short duration storms, but rapidly reduced in efficiency as the return period increased. However, the green roof continued to perform fairly well even under higher return periods if the storm duration was increased. The uncertainty associated with the probability of failure was fairly large for lower return period storms, and was larger for long duration storms than for short duration ones. However, the uncertainty rapidly decreased as the return period increased. The fragility curves show an appropriate level of probability of failure for the >0% and >20% reduction standards, but showed poor performance for higher standards.

Based on the low level of discrepancy between results produced by FORM and those produced by SORM and Monte Carlo simulation, the importance and sensitivity analysis conducted using FORM was appropriate for almost all storms. The importance analysis showed an important distinction between the mechanisms that green roofs use to reduce runoff during short duration and long duration storms. High return period, short duration storms; low return period, short duration storms; and high return period, long duration storms show that infiltration-based variables are most important. However, saturation-based variables are most important for long duration, low return period storms. This discrepancy shows that different mechanisms dominate peak runoff reduction processes during different types of storms. Thus, increasing the depth of soil planting medium can potentially help to reduce the probability of failure of a green roof, but only if the most common storms in the area are long duration storms, in which saturation plays a major role. If short duration 'pop-up' thunderstorms are most common, the most effective way to reduce peak runoff is by appropriate selection of the saturated hydraulic conductivity of the planting medium.

In many municipalities in the United States, a major barrier to green infrastructure implementation is a lack of clearly communicated knowledge about green infrastructure performance, costs, and benefits. The use of fragility curves to convey this type of

information can help bridge this gap and reduce the perceived risk associated with green roofs. Fragility curves can allow municipalities, investors, and designers to better evaluate where and when green roofs can be most effective and to use that understanding to plan for the future. Whether a regulatory or an incentives-based approach is taken, fragility curves provide an additional tool to help municipalities and regional planners in implementing green infrastructure in the urban environment. They also allow for better evaluation of green infrastructure that is already in place, by creating a better understanding of what optimal performance to expect. The generalized approach of this methodology could be easily adapted for multiple types of green infrastructure, failure standards, and available modeling programs.

Future extensions of this work include better understanding the mechanisms governing green roof runoff during winter storms. In particular, the impact of ice and snow on a green roof during these storms was not taken into account in this analysis. Another application could include the impact of inter-storm duration on runoff reduction. Because antecedent moisture has been shown to have an impact on green roof runoff reduction, the inter-storm period could potentially have large repercussions on the probability of failure. Green roofs do require some maintenance in order for them to perform at optimal capacity; studying the impact of maintenance on the probability of failure could further expand the applicability of the model. Finally, the methodology presented in this paper is flexible enough to adapt to different forms of green infrastructure (including rain gardens and bioswales) or different failure criteria (e.g., volume reduction).

REFERENCES

Bai, J., Hueste, M., & Gardoni, P. (2009). Probabilistic assessment of structural damages due to earthquakes for buildings in Mid-America. *Journal of Structural Engineering, 135*(10), 1155-1163.

Baik, J., Kwak, K., Park, S. & Ryu, Y. (2012). Effects of building roof greening on air quality in street canyons. *Atmospheric Environment, 61,* 48-55.

Benedict, M. & McMahon, E. (2006). *Green infrastructure: Linking landscapes and communities*. Washington, DC: Island Press.

Carter, T., & Rasmussen, T. (2006). Hydrologic behavior of vegetated roofs. *Journal of the American Water Resources Association, 42*(5), 1261-1274.

Carter, T. & Jackson, C. (2007). Vegetated roofs for stormwater management at multiple spatial scales. *Landscape and Urban Planning, 80*, 84-94.

Center for Neighborhood Technologies (CNT). (2010). Green infrastructure benefits and practices: Green roofs. In *The value of green infrastructure: A guide to recognizing its environmental, economic and social benefits* (Section 2.1). Retrieved from http://www.cnt.org/repository/gi-values-guide.pdf.

Christensen, D. (2008). *Hydrologic distributed modeling approach for quantifying the hydrologic impacts of rain gardens in urban catchments* (Masters thesis). University of Illinois at Urbana-Champaign, Urbana, IL.

Choi, N. & Schmidt, A. (2013). Elemental unit hydrograph approach to estimate infiltration and inflow in urban area. *Proceedings of ASCE EWRI World Environmental & Water Resource Congress* (pp. 19-23). Cincinatti, Ohio: ASCE.

City of New York Department of Environmental Protection. (2014). *Report for post-construction monitoring green infrastructure neighborhood demonstartion areas.* New York: City of New York Bureau of Sustainability.

Clean Water Education Partnership (CWEP). (2015). *Why is stormwater a problem?* Retrieved from http://www.nccwep.org/stormwater/stormwater101/stormwater_problem.php.

Davis, A. (2008). Field performance of bioretention: Hydrology impacts. *Journal of Hydrologic Engineering, 13*(2), 90-95.

DeLisle, J., Grissom, T., & Högberg, L. (2013). Sustainable real estate: An empirical study of the behavioral response of developers and investors to the LEED rating system. *Journal of Property Investment and Finance, 31*(1), 10-40.

Deutsch, B., Whitlow, H., Sullivan, M., & Savineau, A. (2005). Re-greening Washington, DC: A green roof vision based on environmental benefits for air quality and storm water management. p. 379–384**.** *3rd North American Green Roof Conference: Greening rooftops for sustainable communities* (pp. 379-384).Washington, DC: Green Roofs for Healthy Cities.

DHI Software. (2007). *MIKE SHE user manual: Reference guide (Volume 2).* Retrieved from http://www.hydroasia.org/jahia/webdav/site/hydroasia/shared/Document_public/Project/Manuals/WRS/MIKE_SHE_ReferenceGuide.pdf.

Dietz, M., & Clausen, J. (2005). A field evaluation of rain garden flow and pollutant treatment. *Water, Air and Soil Pollution, 167*, 123-138.

Dunnett, N., & Kingsbury, N. (2008). *Planting green roofs and living walls* (2nd ed.). Portland, Oregon: Timber Press.

Dunnett, N, & Nolan, A. (2004). The effect of substrate depth and supplementary watering on the growth of nine herbaceous perennials in a semi-extensive green roof. *Acta Horticulturae*, *643,* 305–309.

Food and Agriculture Organization. (2015). *Chapter 3- Meteorological data.* Retrieved from Crop evapotranspiration- Guidelines for computing crop water requirements: http://www.fao.org/docrep/x0490e/x0490e07.htm#TopOfPage.

Frazer L. (2005). Paving paradise. *Environmental Health Perspectives*, *113*, 457–462.

Freeman, J. & Farber, D. (2005). Modular environmental regulation. *Duke Law Journal, 54,* 795-798.

Gagliano, A., Detommaso, M., Nocera, F., & Evola, G. (2015). A multi-criteria methodology for comparing the energy and environmental behavior of cool, green and traditional roofs. *Building and Environment, 90*, 71-81.

Gallo, C., Moore, A., & Wywrot, J. (2012). Comparing the adaptability of infiltration based BMPs to various U.S. Regions. *Landscape and Urban Planning, 106*, 326-335.

Gardoni, P. (2014). Lecture on *Reliability analysis (Importance and sensitivity).* Personal collection of P. Gardoni, University of Illinois at Urbana-Champaign, Urbana, Illinois.

Getter, K., & Rowe, D. (2006). The role of extensive green roofs in sustainable development. *HortScience, 41*(5), 1276-1285.

Hanna Holloway, H. (2009). *Monitoring the hydrologic and water-quality effects of a simple-intensive green roof* (unpublished master's thesis). University of Illinois at Urbana-Champaign, Urbana, Illinois.

Hanna Holloway, N., Werth, C., & Schmidt, A. (2009). Monitoring the hydrologic effects of an extensive green roof. *World Environmental and Water Resources Congress:Great Rivers* (pp. 1382-1399). Kansas City, MO: ASCE.

Hasofer, A. & Lind, N. (1974). Exact and invariant second-moment code format. *Journal of the Engineering Mechanics Division, 100* (1), 111-121.

Hilten, R., Lawrence, T., & Tollner, E. (2008). Modeling stormwater runoff from green roofs with HYDRUS-1D. *Journal of Hydrology, 358*, 288-293.

Holloway, C., Strickland, C., Gerrard, M. & Firger, D. (2014). Solving the CSO conundrum: Green infrastructure and the unfulfilled promise of federal-municipal cooperation. *Harvard Environmental Law Review, 38*, 335-370.

Holman-Dodds, J., Bradley, A., & Potter, K. (2003). Evaluation of hydrologic benefits of infiltration based urban stormwater management. *Journal of the American Water Resources Association, 39*(1), 205-215.

Illinois State Water Survey. (2009). *Average wind speed in Illinois*. Retrieved from Illinois State Water Survey Prairie Research Institute: http://www.isws.illinois.edu/atmos/statecli/wind/wind.htm.

Illinois State Water Survey. (2010). *Official 1981-2010 normals for Urbana, IL.* Retrieved from Illinois State Water Survey Prairie Research Institute: http://www.isws.illinois.edu/atmos/statecli/newnormals/normals.USC00118740.txt.

Jaber, F. and Shukla, S. (2012). MIKE SHE: Model use, calibration and validation. *Transactions of the ASABE, 55* (4), 1479-1489.

Jaffe, M., Zellner, M., Minor, E., Gonzalez-Meler, M., Cotner, L., Massey, D., . . . Wise, S. M. (2010). *Using green infrastructure to manage urban stormwater quality: A review of selected practices and state programs.* Illinois EPA.

Jarrett, A., Hunt, B., & Berghage, R. (2007). Evaluating a spreadsheet model to predict green roof stormwater retention. *Proceedings of the second National Low Impact Development Conference* (pp. 252-259). Wilmington, NC: ASCE.

Jones, K. (2009). Being green doesn't need to be taxing: How New York State Law is a vanguard for using green infrastructure. *Pace Law Review, 29,* 499-509.

Klinkenborg, V. (May 2009). Green roofs. *National Geographic.* Retrieved from http://ngm.nationalgeographic.com/2009/05/green-roofs/klinkenborg-text.

Kondo, M., Low, S., Henning, J., & Branas, C. (2015). The impact of green stormwater infrastructure on surrounding health and safety. *American Journal of Public Health, 105*(3), 114-121.

Kristensen, K., & Jensen, S. (1975). A model for estimating actual evapotranspiration from potential evapotranspiration. *Nordic Hydrology, 6*(3), 170-188.

Li, Y. & Babcock, R. (2014). Green roof hydrologic performance and modeling: A review. *Water Science and Technology, 69*(4), 727-738.

Malina, C. (2011). Up on the Roof: Implementing Local Government Policies to Promote and Achieve the Environmental, Social, and Economic Benefits of Green Roof Technology. *Georgetown International Law Review, 23*(3), 437-463.

Marasco, E., Hunter, B., Culligan, P. Gaffin, S. & McGillis, W. (2014). Quantifying evapotransipiration from urban green roofs: A comparison of chamber measurements with commonly used predictive methods. *Environ. Sci. Technol.*, *48* (17), 10273–10281.

Mentens, J., Raes, D., & Hermy, M. (2005). Green roofs as a tool for solving the rainwater runoff problem in the urbanized 21st century?. *Landscape and Urban Planning*, *77*, 21–226.

Moran, A., Hunt, B., & Smith . J. (2005). Hydrologic and water quality performance from green roofs in Goldsboro and Raleigh, North Carolina. *Third Annual Greening Rooftops for Sustainable Communities Conference, Awards and Trade Show* (pp. 4–6). Washington, DC: Green Infrastructure Foundation.

Moriasi, D., Arnold, J., Van Liew, M., Bingner, R., Harmel, R., & Veith, T. (2007). Model evalutaion guidelines for systematic quantification of accuracy in watershed simulations. *Journal of the American Society of Agricultural and Biological Engineers, 50*(3), 885-900.

Nagase, A. & Dunnett, N. (2010). Drought tolerance in different vegetation types for extensive green roofs: Effects of watering and diversity. *Landscape and Urban Planning, 94,* 318-327.

National Climatic Data Center. (2014). *Global Historical Climatological Network – Daily summaries* [Data file for Urbana, IL by request]. Retrieved from http://www.ncdc.noaa.gov/cdo-web/datasets#GHCND.

National Renewable Energy Laboratory. (1990). *The solar radiation data manual for flat-plate and concentrating collectors for Peoria, IL.* Retrieved from Renewable Resource Data Center: http://rredc.nrel.gov/solar/old_data/nsrdb/1961-1990/redbook/sum2/14842.txt.

Niachou, A., Papakonstantinou, K., Santamouris, M., Tsangrassoulis, A., & Mihalakakou, G. (2001). Analysis of the green roof thermal properties and investigation of its energy performance. *Energy and Buildings, 33,* 719-729.

Nikel, D., Schoenfelder. W., Medearis, D., Dolowitz, D., Keeley, M., & Shuster, W. (2014). German experience in managing stormwater with green infrastructure. *Journal of Water Resources Planning and Management, 57*(3), 403-423.

Oak Ridge National Lab. (2000). *Global Leaf Area Index field measurements, 1993-2000* [Data File]. Retrieved from http://daac.ornl.gov/cgi-bin/dsviewer.pl?ds_id=584.

Obeid, N. (2014). *Low impact development in urban areas for integrated watershed management across scales* (unpublished doctoral dissertation). University of Illinois at Urbana-Champaign, Urbana, IL.

Oberndorfer, E. Lundholm, J. Rass, B., Coffman, R., Doshi, H., Dunnett, N., Gaffin, S., Kohler, M., Liu, K. & Rowe, B. (2007). Green roofs as urban ecosystems: Ecological structures, functions and services. *BioScience*, *57* (10), 823-833.

Rackwitz, R. & Fiessler, B. (1978). Structural reliability under combined load sequences, *Computers and Structures*, *9*(8), 489-494.

Santamouris, M. (2015). Regulating the damaged thermostat of the cities: Status, impacts and mitigation challenges. *Energy and Buildings, 91,* 43-56.

Sakia, R. (1992). The Box-Cox transformation technique: A review. *The Statistician, 41*, 169-178.

Sonne, B. (2014). Managing stormwater by sustainable measures: Preventing neighborhood flooding and green infrastructure implementation in New Orleans. *Tulane Environmental Law Journal, 27,* 323-350.

State of Illinois v. MWRDGC, 11 C8859 (US District Court for the Northern District of Illinois 2014).

Store, E. & Kalisz, P. (1991). On the maximum extent of tree roots. *Forest Ecology and Management, 46,* 59-102.

The Conservation Fund. (2011). *What is Green Infrastructure?* Retrieved from http://www.greeninfrastructure.net/content/definition-green-infrastructure.

Thomspson, B. (2010). *The green roof at the Minnesota Landscape Arboretum.* Retrieved from http://www.arboretum.umn.edu/green_roof.aspx.

Trinh, D. & Chui, T. (2013). Assessing the hydrologic restoration of an urbanized area via integrated distributed hydrological model. *Hydrology and Earth System Sciences Discussions, 10*, 4099-4132.

van Genutchen, M. (1980). A closed form equation for predicting the hydraulic conductivity of unsaturated soils. *Soil Science Society of America Journal, 12*(3), 513-522.

Vanuytrecht, E., Van Mechlen, C., Van Meerbeek, K., Willems, P., Hermy, M., & Raes, D. (2014). Runoff and vegetation stress of green roofs under different climate change scenarios. *Landscape and Urban Planning, 122*, 68-77.

VanWoert, N., Rowe, D., Andresen, J., Rugh, C., Fernandez, R., & Xiao, L. (2005). Green roof retention: Effects of roof surface, slope and media depth. *Journal of Environmental Quality, 34*, 1036-1044.

Versini, P., Ramier, D., Berthier, E., & de Gouvello, B. (2015). Assessment of the hydrological impacts of green roof: From building scale to basin scale. *Journal of Hydrology, 524*, 562-575.

Vineyard, D., Ingwersen, W., Hawkins, T., Xue, X., Demke, B., & Shuster, W. (2015). Comparing green and grey insfrastructure using life cycle cost and environmental impact: A rain garden case study in Cincinnati, OH. *Journal of the American Water Resources Association*, 1-19. doi:10.1111/1752-1688.12320.

Virk, G., Jansz, A., Mavrogianni, A., Mylona, A., Stocker, J., and Davies, M. (2015). Microclimatic effects of green and cool roofs in London and their impacts on energy use for a typical office building. *Energy and Buildings, 88,* 214-228.

Wang, R., Eckelman, M., & Zimmerman, J. (2013). Consequential environmental and economic life cycle assessment of green and gray stormwater infrastructures for combined sewer systems. *Environmental Science and Technology, 47*, 11189-11198.

William, R. & Schmidt, A. (2015). Computer-based modeling of impacts of Prunus Africana on groundwater in Northwestern Cameroon. *Journal of Water Resources Planning and Management.* 10.1061/(ASCE)WR.1943-5452.0000549 , A5015003.

Wilson, C., Hunt, W., Winston, R., & Smith, P. (2013). A comparison of runoff quality and quantity from an urban commercial infill Low Impact Development and a conventional development. *World Environmental and Water Resources Congress 2013* (pp. 2910-2923). Cincinnati, OH: ASCE.

Wong, T. (2006). Integrated approach to urban stormwater management. *EWRI World Water and Environmental Congress BMP Technology Symposium: Current and future directions* (pp. 24-36). Salt Lake City, UT: ASCE.

Yan, J., & Smith, K. (1994). Simulation of integrated surface water and groundwater systems - model formulation. *Journal of the American Water Resources Association, 30*(5), 879-890.

Yen, B. & Chow, V. (1980). Design hyetographs for small drainage structures. *Journal of the Hydraulics Division of ASCE, 106* (6), 1055-1076.

Yocca, D. (2002). 2002 Award Winners: Chicago City Hall green roof, Chicago, Illinois. *ASLA online.* Retrieved from http://www.asla.org/meetings/awards/awds02/chicagocityhall.html.